Physiological Measurement

IPEM
Institute of Physics and Engineering in Medicine

TOPICAL REVIEW

System identification: a multi-signal approach for probing neural cardiovascular regulation

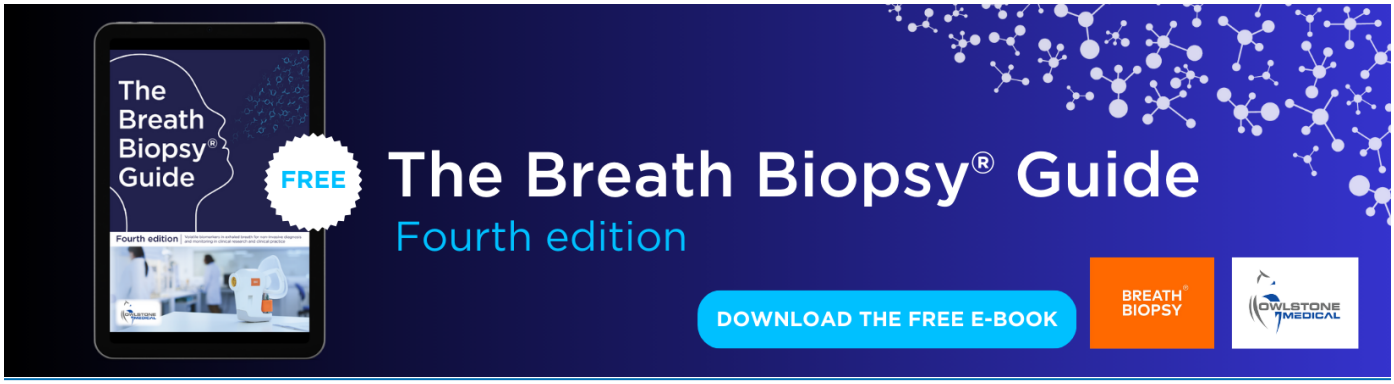

INSTITUTE OF PHYSICS PUBLISHING PHYSIOLOGICAL MEASUREMENT

Physiol. Meas. **26** (2005) R41–R71 doi:10.1088/0967-3334/26/3/R01

TOPICAL REVIEW

System identification: a multi-signal approach for probing neural cardiovascular regulation

Xinshu Xiao[1], **Thomas J Mullen**[2] **and Ramakrishna Mukkamala**[3]

[1] Harvard-MIT Division of Health Sciences and Technology, Massachusetts Institute of Technology, 77 Mass Ave, Cambridge, MA 02139, USA
[2] Medtronic Inc., MS CW320, 7000 Central Avenue NE, Minneapolis, MN 55432, USA
[3] Department of Electrical and Computer Engineering, Michigan State University, 2120 Engineering Building, East Lansing, MI 48824, USA

E-mail: rama@egr.msu.edu

Received 25 August 2004, accepted for publication 19 November 2004
Published 1 February 2005
Online at stacks.iop.org/PM/26/R41

Abstract

Short-term, beat-to-beat cardiovascular variability reflects the dynamic interplay between ongoing perturbations to the circulation and the compensatory response of neurally mediated regulatory mechanisms. This physiologic information may be deciphered from the subtle, beat-to-beat variations by using digital signal processing techniques. While single signal analysis techniques (e.g., power spectral analysis) may be employed to quantify the variability itself, the multi-signal approach of system identification permits the dynamic characterization of the neural regulatory mechanisms responsible for coupling the variability between signals. In this review, we provide an overview of applications of system identification to beat-to-beat variability for the quantitative characterization of cardiovascular regulatory mechanisms. After briefly summarizing the history of the field and basic principles, we take a didactic approach to describe the practice of system identification in the context of probing neural cardiovascular regulation. We then review studies in the literature over the past two decades that have applied system identification for characterizing the dynamical properties of the sinoatrial node, respiratory sinus arrhythmia, and the baroreflex control of sympathetic nerve activity, heart rate and total peripheral resistance. Based on this literature review, we conclude by advocating specific methods of practice and that future research should focus on nonlinear and time-varying behaviors, validation of identification methods, and less understood neural regulatory mechanisms. Ultimately, we hope that this review stimulates such future investigations by both new and experienced system identification researchers.

Keywords: autonomic nervous system, cardiovascular system, heart rate variability, modeling

1. Introduction

It has long been recognized that cardiovascular variables such as heart rate (HR) and arterial blood pressure (ABP) fluctuate on a beat-to-beat basis. Indeed, in the early 18th century when Hales made the first quantitative measurements of ABP, he noted that the inter-beat interval and pressure level varied with the respiratory cycle (Hales 1733). However, prior to the advent of modern digital signal processing in 1965 (Cooley and Tukey 1965), the subtle, beat-to-beat cardiovascular variations were difficult to characterize quantitatively and therefore received little attention. In the 1970s and early 1980s, Kitney, Cohen and their respective co-workers applied power spectral analysis to study the genesis of resting HR variability (e.g., Akselrod *et al* (1981), Hyndman *et al* (1971) and Kitney (1975)). These quantitative studies were among the first to demonstrate that beat-to-beat cardiovascular variability reflects the dynamic interplay between ongoing physiologic perturbations to the circulation and the compensatory response of the cardiovascular regulatory system. Following these pioneering efforts, an explosion of interest commenced in the analysis of beat-to-beat cardiovascular variability (especially HR variability) for the quantitative assessment of cardiovascular regulation. While power spectral analysis has been the workhorse in the field, numerous, more sophisticated analysis techniques have also been applied to characterize the nonlinear and nonstationary fluctuations in a single cardiovascular variable (see, e.g., reviews in Mainardi *et al* (2002) and Mansier *et al* (1996)). These single signal analysis techniques have provided much insight into the nature of the variability and cardiovascular regulatory function. However, the multi-signal analysis approach of system identification may be even more illuminating, as it can provide a quantitative characterization of the cardiovascular regulatory mechanisms responsible for coupling the beat-to-beat variability between signals rather than merely the variability that is elicited. Thus, beginning with the seminal studies of Cohen, Cerutti and their respective co-workers in the mid to late 1980s (e.g., Akselrod *et al* (1985) and Baselli *et al* (1986, 1988)), system identification has become an increasingly popular approach for quantitatively probing cardiovascular regulation.

In this topical review, we aim to provide an overview of applications of system identification to beat-to-beat variability for the quantitative characterization of cardiovascular regulatory mechanisms. While the assessment of local autoregulatory mechanisms has recently become a subject of interest (see, e.g., review in Panerai (1998)), we focus here on the more established system identification applications for probing global regulatory mechanisms mediated by the autonomic nervous system. Our review is specifically aimed at the reader with some knowledge of both signals and systems theory and cardiovascular physiology. We begin by briefly summarizing basic principles and motivating concepts (section 2). We then review the practice of system identification in the context of studying neural cardiovascular regulation (section 3) and describe important contributions that have been made in the field during the past two decades (section 4). We conclude by recommending specific methods of practice and future research directions (section 5).

2. Basic principles

We start this section with brief descriptions of the normal functioning of the neural cardiovascular regulatory system and conditions for which this functioning is altered. We then review alternative methods for probing neural regulatory functioning and describe their limitations so as to motivate the use of system identification.

2.1. Neural cardiovascular regulation

2.1.1. Physiology. Global or extrinsic cardiovascular regulation aims to maintain blood pressures within a narrow range via multiple feedback and control systems in order to protect blood flow to the brain, heart, and other vital organs. The autonomic nervous system is principally responsible for extrinsic regulation over short time scales of seconds to minutes usually through mediation of the arterial and cardiopulmonary baroreflex mechanisms. The arterial baroreflex, which is the much more understood mechanism, operates as follows. ABP is sensed via baroreceptors that lie in the carotid sinus and aortic arch and then conveyed to the brainstem via afferent nerve fibers. The brain responds in an attempt to keep ABP near its desired value by communicating with (1) the sinoatrial (SA) node via efferent parasympathetic and β-sympathetic nerve fibers to adjust HR; (2) the ventricles via efferent β-sympathetic nerve fibers to adjust ventricular contractility (VC); (3) the arterioles via efferent α-sympathetic nerve fibers to adjust total peripheral resistance (TPR) and (4) the veins via efferent α-sympathetic nerve fibers to adjust systemic venous unstressed volume (SVUV). For example, the net feedback response of the arterial baroreflex to a reduction in ABP would be an increase in HR, VC and TPR and a decrease in SVUV. These adjustments would, in turn, increase ABP back towards its desired value via mechanical feedforward effects. The cardiopulmonary baroreflex operates analogously except that its sensory receptors, which reside mostly in the cardiac chambers but also in the walls of the pulmonary artery, seem to be very responsive to changes in right atrial pressure (RAP) (Desai *et al* 1997, Raymundo *et al* 1989). This mechanism appears to be more focused on the maintenance of ABP rather than RAP, as its net response to a reduction in RAP may include an increase in TPR and HR in humans (Desai *et al* 1997, Mancia and Mark 1983, Raymundo *et al* 1989). Proper functioning of the rapid nervous control mechanisms is most critical during physiologic perturbations such as postural changes and exercise. However, they contribute little to blood pressure regulation over longer time scales, because their receptors may eventually adapt to the pressure levels to which they are exposed. See, for example, Guyton and Hall (1996) for more thorough accounts of the baroreflex systems and descriptions of other neural regulatory mechanisms that are activated only during periods of hemodynamic stress (e.g., arterial chemoreflex).

2.1.2. Disease. Aberrant neural cardiovascular regulatory function can result from disease and environmental changes. Hypertension (HTN) is perhaps the most prominent and prevalent example of a disease of cardiovascular regulation. While HTN is likely to be due to maladies of long-term regulatory mechanisms (Guyton and Hall 1996), malfunctioning neural regulatory mechanisms also appear to contribute (Moreira *et al* 1992). Congestive heart failure (CHF) is another prevalent disease affecting short-term regulation. Although the primary problem of CHF is with pumping function, a hallmark of this disease is hyperactivity of the sympathetic nervous system (Mark 1995). Examples of other common diseases affecting short-term regulation include diabetes mellitus and Parkinson's disease. Patients with these disease processes frequently suffer from postural hypotension due to blunted autonomic nervous functioning (Goldstein *et al* 2002, Jermendy 2003). Indeed, the presence of postural hypotension in patients with diabetes mellitus may be associated with high mortality (Ewing *et al* 1976). Interestingly, exposure to actual or simulated microgravity has also been shown to alter rapid cardiovascular regulatory function (Hasser and Moffitt 2001). These alterations, often referred to as cardiovascular deconditioning, likely contribute to the postural hypotension commonly observed in astronauts upon return from spaceflight (Buckey *et al* 1996). Note that a measure of the utility of system identification methods for characterizing cardiovascular regulatory function is the capacity of these methods to detect, quantify and

monitor the deleterious changes in function seen as a result of disease (or environment) and subsequent improvements seen with therapies.

2.2. Probing neural cardiovascular regulation

2.2.1. Conventional methods. Because of the significance of neural cardiovascular regulation in health and disease, numerous methods have been developed for its measurement. The conventional methods involve perturbing the circulation with an external stimulus, measuring the regulatory response and usually, but not always, plotting the measured response as a function of the stimulus. The external stimuli that have been employed may be broadly classified as selective or nonselective (Mancia and Mark 1983). In principle, selective stimuli excite and permit the study of one particular feedback mechanism (e.g., arterial baroreflex) without any confounding contribution from other feedback mechanisms (e.g., cardiopulmonary baroreflex). Common examples of this type of stimuli include carotid sinus pressure control and vasoactive drugs. (The latter stimulus is often utilized for study of the arterial baroreflex control of HR). However, these stimuli open or disturb the feedback loop and thereby preclude study during normal physiologic conditions. Moreover, the tenet that only one feedback mechanism has been perturbed may not be valid. Nonselective stimuli excite all feedback mechanisms simultaneously. The archetypical example of this kind of stimuli is upright tilting. The advantage of employing nonselective stimuli is that they can preserve normal closed-loop operation. However, the relative contribution of each feedback mechanism to the total system response cannot be distinguished with a simple plotting analysis. Another major limitation of the conventional methods is that they only measure the steady-state compensatory response to the external stimulus. However, neural regulatory mechanisms are not simply static systems which can be described with algebraic equations but are rather complex systems with memory that mandate description with differential equations (i.e., dynamical systems). Thus, the conventional methods neglect the characterization of important quantitative information such as time constants and delays.

2.2.2. Quantitative analysis of beat-to-beat cardiovascular variability. Cardiovascular measurements such as HR, ABP, RAP and stroke volume (SV) fluctuate on a beat-to-beat basis. These subtle variations are not simply noise in the classical sense but rather representative of the dynamic interplay between naturally occurring perturbations to the circulation and the negative feedback response of the cardiovascular regulatory system. The most prominent example of such perturbations is respiratory activity, which mechanically induces inter-beat variations in intrathoracic pressure thereby altering venous return, RAP and ABP thereafter. Respiratory activity also directly perturbs HR via a neural coupling between the respiratory and HR control centers in the brain (Saul and Cohen 1994). While these HR variations further modulate RAP and ABP, note that the neurally mediated RAP changes, in particular, may offset the mechanically induced RAP changes. (That is, the purpose of the direct neural coupling mechanism may be to maintain RAP during respiration.) Another example of resting perturbations is the autoregulation of local vascular beds, which alters TPR on a beat-to-beat basis and thus ABP and RAP. The resulting ABP and RAP changes, in turn, induce compensatory variations in HR, SV and TPR via the arterial and cardiopulmonary baroreflex systems. (See, for example, the reviews in Baselli *et al* (2002) and Miyakawa *et al* (1984) for a thorough description of the complex physiologic mechanisms responsible for generating beat-to-beat hemodynamic variability.) Indeed, quantitative analysis of short-term, beat-to-beat information in cardiovascular signals is an attractive alternative for probing neural regulatory function, as an external perturbing stimulus may not be necessary.

Over the last three decades, investigators have successfully applied numerous quantitative techniques for the analysis of beat-to-beat variability in cardiovascular signals. Even simple statistics indicating only the range of variation of a particular signal, such as the standard deviation and histogram, have proven to be useful. For example, Kleiger *et al* demonstrated that a decreased standard deviation of HR variability was associated with increased mortality in a large number of acute myocardial infarction patients (Kleiger *et al* 1987). However, the significance of beat-to-beat cardiovascular variability only became fully appreciated when techniques that could measure both the range and speed of the variations in a signal were applied. Examples of such techniques include the autocorrelation function and its Fourier transform, the power spectrum. One of the earliest attempts to investigate beat-to-beat variability with such techniques was made by Sayers (1973). He specifically employed power spectral analysis to characterize short-term HR fluctuations. He found not only a significant HR fluctuation at the respiratory frequency (i.e., the well-known respiratory sinus arrhythmia (RSA) phenomena) but also significant variability at lower frequencies, which was subsequently attributed to vasomotor activity (Akselrod *et al* 1981, 1985, Kitney 1975). Akselrod *et al* followed this work by demonstrating for the first time that power spectral analysis of resting HR could provide specific measures of neural regulatory function (Akselrod *et al* 1981). These researchers showed in a conscious canine model that high frequency HR fluctuations ($\geqslant$0.15 Hz) were governed exclusively by the parasympathetic nervous system, whereas the lower frequency HR fluctuations were jointly mediated by the β-sympathetic and parasympathetic nervous systems. These important findings were later verified in humans (Pomeranz *et al* 1985). Subsequent investigators have identified clinical correlates of HR variability spectral indices (e.g., low frequency (LF) and high frequency (HF) power) and employed more sophisticated, nonlinear (e.g., Lyapunov exponents, Kolmogorov entropy) and nonstationary (e.g., short-time Fourier transform, wavelets) techniques to elucidate further the complex nature of short-term as well as long-term HR variability (see, e.g., reviews in Mainardi *et al* (2002) and Malik and Committee (1996)).

While such single signal analysis techniques have clearly contributed to the understanding of cardiovascular regulatory functioning, these techniques are significantly limited in that they characterize only the output response of the system under study rather than the system itself. This limitation can be made more lucid through the following example. Let $y(t)$ be a signal for analysis which may represent, for example, instantaneous HR. Now, suppose that $y(t)$ is generated according to the convolution of an input signal $u(t)$, which may represent, for example, respiratory activity, and an impulse response $h(t)$, which characterizes the direct neural coupling mechanism between $u(t)$ and $y(t)$ (see equation (1)). Thus, it is $h(t)$ that should actually be sought for characterization. However, if only $y(t)$ is available for analysis, it is generally not possible to determine $h(t)$ uniquely (e.g., convolution commutes). In other words, alterations in $y(t)$ (HR) occurring from one time interval to the next may be due to changes in $h(t)$ (autonomic nervous functioning) and/or variations in $u(t)$ (respiratory effort). On the other hand, if a simultaneous measurement of the input signal $u(t)$ is obtained, then the problem now becomes: given $u(t)$ and $y(t)$, what is $h(t)$? This is the system identification problem, which is soluble under more general conditions (see below). (Note that this discussion is only exemplary and not intended to imply that the cardiovascular regulatory system is perfectly linear and time invariant (LTI) or that system identification is only applicable to such systems.) Hence, system identification provides a means to characterize the neural regulatory mechanisms responsible for generating the beat-to-beat variability rather than simply the variability that is generated. Table 1 indicates the advantages of the multi-signal approach of system identification over other methods for probing neural cardiovascular regulation.

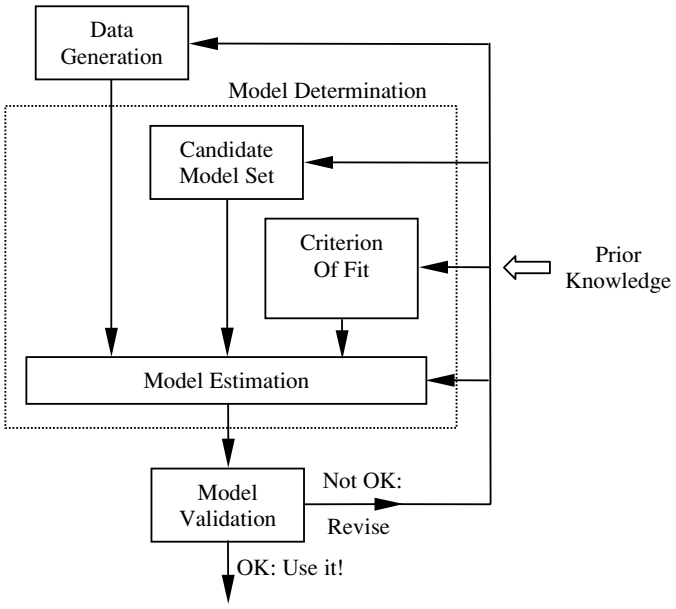

Figure 1. The system identification method loop. Adapted from Ljung (1999).

Table 1. Disadvantages of popular methods for probing neural cardiovascular regulatory mechanisms with respect to system identification.

Method	Disadvantages
Application of selective external perturbations (e.g., vasoactive agents)	Opens or disturbs the feedback loop; measures only the steady-state system response
Application of nonselective external perturbations (e.g., upright tilting)	Cannot distinguish contributions of different regulatory mechanisms to the system response; measures only the steady-state system response
Single signal analysis of beat-to-beat variability (e.g., HR variability analysis)	Cannot distinguish contributions of input and regulatory mechanism to the system response

3. The system identification method

The control systems engineering community is largely responsible for developing and advancing the field of system identification. Their initial contributions began shortly after the establishment of modern control theory in the 1960s. At present, the field is very mature and several comprehensive textbooks on the subject matter exist (e.g., Ljung (1999), Marmarelis and Marmarelis (1978) and Soderstrom and Stoica (1988)). In this section, we summarize the practice of system identification specifically in the context of probing neural cardiovascular regulation.

The system identification method is an iterative process consisting of three basic steps: (1) data generation, (2) model determination and (3) model validation (see figure 1). If the model is not validated, then steps (1) and/or (2) are adjusted and the ensuing steps are repeated until successful model validation is achieved. *A priori* knowledge should be injected in this process wherever possible.

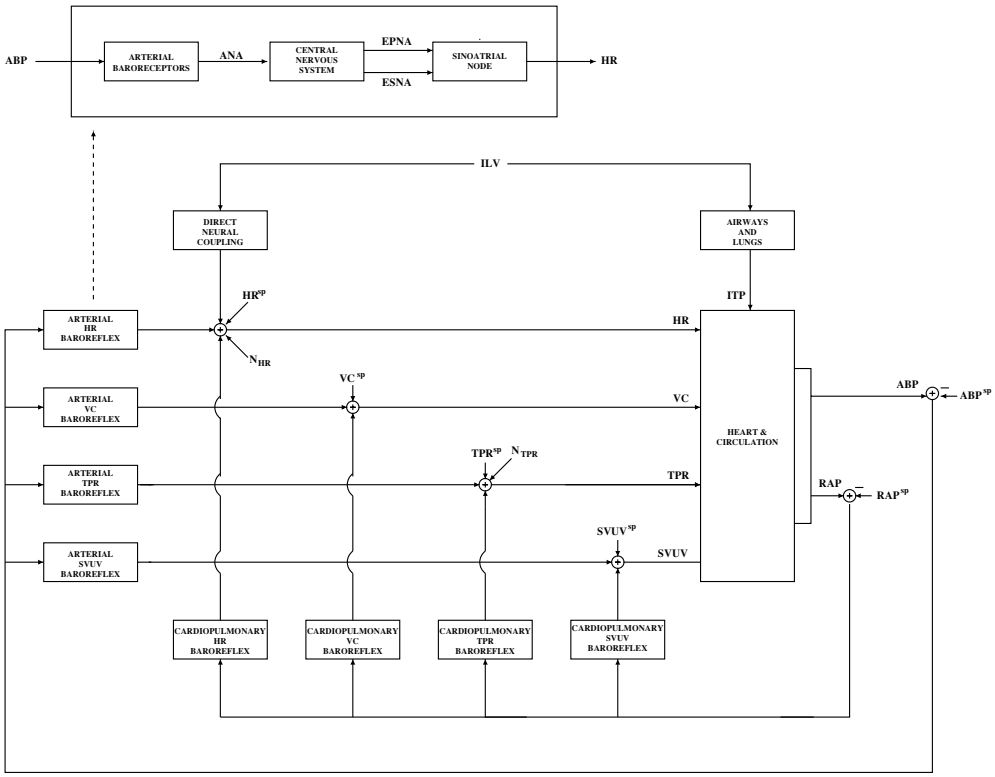

Figure 2. Block diagram of key input and output signals and physiologic coupling mechanisms normally involved in cardiovascular regulation over time scales of seconds to minutes. ABP is arterial blood pressure; RAP, right atrial pressure; HR, heart rate; VC, ventricular contractility; TPR, total peripheral resistance; SVUV, systemic venous unstressed volume; ILV, instantaneous lung volume; ITP, intrathoracic pressure; ANA, afferent nervous activity; EPNA, efferent parasympathetic nervous activity; ESNA, efferent sympathetic nervous activity; sp, setpoint; N_{TPR}, autoregulation of local vascular beds and N_{HR}, source of $1/f$ HR fluctuations.

3.1. Data generation

3.1.1. Measured signals. As described above, neural cardiovascular regulation is a highly complex multi-input, multi-output process operating in closed-loop. The block diagram in figure 2 illustrates the key input and output signals and physiologic coupling mechanisms (blocks) that are normally involved. If the beat-to-beat variability in all these signals were measured, then, in principle, a comprehensive, dynamical characterization of all of the neurally mediated coupling mechanisms may be obtained.

Continuous ABP may be easily measured either invasively with a strain gauge in fluid contact with a peripheral artery or noninvasively via, for example, arterial tonometry (Kenner 1988) and finger-cuff photoplethysmography (Imholz *et al* 1998). Instantaneous HR may be even more easily determined by detecting the *R*-waves of a surface ECG lead. Respiratory activity may also be conveniently monitored either in terms of intrathoracic pressure via an esophageal balloon (Mead and Gaensler 1959) or in terms of instantaneous lung volume (ILV) via chest–abdomen inductance plethysmography. RAP may be measured, but with a considerably higher degree of invasiveness, by placing a strain gauge in fluid contact with the right atrium via a pulmonary artery catheter. Both afferent and efferent neural signals may

be measured with electrodes, but very invasive and technically challenging procedures are required to do so. On the other hand, continual variations in TPR, VC and SVUV are not directly measurable. However, it may be possible to derive beat-to-beat measurements of TPR from central ABP alone (Bourgeois *et al* 1974) or with peripheral ABP and instantaneous aortic flow (e.g., Mukkamala *et al* (2003)). The latter signal may be measured in animals by surgically implanting an ultrasonic flow probe around the aorta or in humans by directing a noninvasive Doppler ultrasound probe towards the aortic valve (e.g., Eriksen and Walloe (1990)). It may also be possible to derive beat-to-beat changes in VC from simultaneous measurements of ventricular pressure and volume (e.g., Senzaki *et al* (1996)). The ventricular volume signal may be measured invasively with a conductance catheter (Baan *et al* 1984) or ultrasonic crystals sutured to the ventricle (Ellis *et al* 1956) or noninvasively with echocardiographic techniques. Finally, no technique has been proposed to derive SVUV fluctuations from other directly measurable signals.

Thus, it is not practical (or possible) to obtain simultaneously beat-to-beat measurements of most (or all) of the key signals involved in neural cardiovascular regulation, and a choice of the specific signals to be measured must be made. This choice invariably reflects a trade-off between the effort and feasibility of measuring the signal in the particular experiment (e.g., animal or human) and the importance of the particular neural regulatory mechanism to be investigated. It should therefore not be surprising that much of the previous system identification studies have involved only the analysis of ABP and HR. With these measurements, the arterial HR baroreflex mechanism may be characterized by identifying the dynamic coupling from ABP fluctuations to HR fluctuations. Note that this coupling actually lumps together the functioning of the baroreceptors, autonomic nervous system and SA node (see figure 2). To characterize each of these individual components or other neural regulatory mechanisms in the block diagram of figure 2, additional beat-to-beat measurements would be needed. In general, if n signals are available for analysis, then $n(n-1)$ causal physiologic coupling mechanisms (some of which represent nonregulatory mechanisms) may be identified.

3.1.2. Informative data. The data generation step not only involves choosing which signals are to be measured and by what means but also designing the experiments such that the measured signals permit reliable model determination in the subsequent step. In the identification of linear models (see below), the measured data should be 'sufficiently informative' such that the model determination process results in a unique model. More specifically, for nonparametric models, which do not assume any particular structure (see below), the input signal should contain all the frequencies of the system under study. For parametric models, which assume a particular structure (see below), the input signal should contain at least as many frequency components as the number of parameters characterizing the system in question. Since the system frequency bandwidth or number of system parameters is generally unknown *a priori*, the measured input signal would ideally be a white noise process of uniform spectral density. For multi-input systems, sufficiently informative also means that the input signals are different enough from each other. For example, if the input signals differ only by a scale factor, then it would be impossible to distinguish the contribution of each input to the output. Ideally, the measured input signals would also be uncorrelated. However, spontaneous, beat-to-beat variations in neural regulatory input signals such as ABP and RAP are both colored and correlated processes due to feedback and mechanical couplings. While spontaneous variability may nevertheless be sufficiently informative for a particular identification task, the experimental design may include the application of external randomized perturbations in order to ensure enough information or, at least, enhance the measured information. Moreover, for reasons described below, the statistical requirements of

the measured inputs can even be more stringent in the identification of nonlinear models (e.g., zero-mean white noise processes defined by Gaussian or normal distributions). Thus, such external perturbations can some times be necessary for the accurate identification of these models.

3.1.3. Preprocessing. Once the experiments have been completed, the measured data usually require preprocessing before the model determination step can be executed. Perhaps, the most significant aspect of preprocessing in the context of probing neural regulatory mechanisms is the derivation of input and/or output signals from the measured data. The archetypical example is the formation of an instantaneous HR signal from a surface ECG measurement (e.g., Berger *et al* (1986)). Additional examples are provided above. Another important aspect of preprocessing is the choice of the sampling frequency. If the sampling frequency is chosen to be too low relative to the bandwidth of the particular system under study, then it will not be possible to characterize completely the dynamical properties of that system. On the other hand, if the sampling frequency is chosen to be too high, then unnecessary measurement noise will be introduced in the data. Since the system bandwidth is usually unknown *a priori*, it is generally recommended that the chosen sampling frequency be about ten times the expected bandwidth of the system in question (Ljung 1999). In this way, uncertainty in the expected bandwidth will likely not compromise the information in the data. (For example, in the identification of the arterial HR baroreflex, the expected bandwidth is about 0.5 Hz. Thus, sampling the measured ABP and HR signals at $\sim$3 Hz would satisfy this recommendation. Typically, these signals are sampled by first forming sequences of beat-to-beat values (e.g., systolic blood pressure) and then interpolating between these values to create time series.) A final aspect of preprocessing is the removal of measurement noise such as high frequency disturbances, baseline wander, missing data and outliers. Noise removal may be achieved with, for example, filtering or splining techniques. Note that imperfect noise removal can be dealt within the model determination step, because the models not only include a deterministic component but also a stochastic component (see below). However, nonstationary noise (e.g., linear trends or outliers) should be treated as much as possible prior to model determination, as the stochastic components are usually assumed to be stationary.

3.2. Model determination

3.2.1. Overview. Model determination is the step in which the model that 'best' couples the input–output data is selected. To make this step tractable, a candidate set of models must first be established. Then, the optimal model in the set is usually determined by minimizing the variance of the unobserved stochastic disturbance. This least squares estimation approach is appropriate when the unobserved disturbance is normally distributed, which may often be the case due to central limit theorem arguments. However, the least squares criterion may not always be appropriate, such as when the unobserved disturbance is characterized by more heavy tailed distributions (e.g., significant presence of outliers). In these cases, other minimization criteria (e.g., mean absolute error) should be employed.

3.2.2. Linear versus nonlinear. A key question that must be addressed in establishing a set of candidate models is: can the system under study be represented with a linear model? The answer is generally no for neural cardiovascular regulatory mechanisms, as their high degree of complexity must mandate nonlinear behaviors. Indeed, previous experimental investigations have reported nonlinearities such as baroreflex saturation and hysteresis (Mancia and Mark 1983) as well as cross talk between the arterial and cardiopulmonary baroreflex mechanisms

(Pawelczyk and Raven 1989, Victor and Mark 1985). Nevertheless, linear models may be preferable to nonlinear models, because they are much more intuitive and may therefore be more useful in gaining insight into neural regulatory functioning (see below). Moreover, linear models may be nearly valid when applied to beat-to-beat variability elicited spontaneously at rest or with low amplitude random excitation, as the fluctuations in the measured signals are relatively small (i.e., Taylor series-like approximation). Many of the nonlinear behaviors that have been observed have been elicited under extreme experimental conditions. Indeed, many studies demonstrating nonlinear couplings give results consistent with linear responses for small perturbations (e.g., Bertinieri *et al* (1988), Hirsch and Bishop (1981) and Levison *et al* (1966)). Thus, linear models of neural regulatory mechanisms should be thought of as approximating small signal system behavior around a given operating point. They should not be assumed to be indicative of small signal system behavior around a significantly different operating point. Nonlinear models are needed to characterize small signal system behavior fully and to illuminate large signal system behavior. Finally, we note that the utilization of linear models in the presence of significant nonlinearity may, at least, provide a partial characterization of system behavior.

3.2.3. Stationary versus nonstationary. Another key question that must be resolved in establishing a candidate set of models is: can the system under study be regarded as stationary? That is, can the system and unobserved disturbances be respectively represented with time-invariant equations and statistics? Again, the answer is generally no for the highly complex neural regulatory system, as it is well known that sympatho-vagal balance shifts, for example, upon assuming the upright posture or initiation of exercise (Guyton and Hall 1996). However, time-invariant models may be nearly valid when the data are collected during short time periods of stable, unchanging experimental conditions. On the other hand, time-varying models that assume piece-wise stationarity are needed to study neural regulatory functioning during transient events such as postural changes or acute hemorrhage.

3.2.4. Linear and time-invariant models. If the system to be identified is regarded as LTI, then the system input $u(t)$ may be mapped to the system output $y(t)$ according to the convolution equation:

$$y(t) = \sum_{i=-\infty}^{\infty} h(i)u(t-i) + e(t) = \sum_{i=-\infty}^{\infty} u(i)h(t-i) + e(t), \tag{1}$$

where t is discrete time, $h(t)$ is the system impulse response and $e(t)$ is an unobserved, stochastic process that is uncorrelated to $u(t)$. The term $e(t)$ may represent, for example, measurement noise and/or omitted inputs. Note that the impulse response not only completely defines an LTI system but also represents the system response to an arbitrarily narrow, unit-area input applied at time zero.

To specify further the candidate set of LTI models, a choice must be made between the use of nonparametric or parametric representations of the impulse response or its Fourier transform, the transfer function. If a nonparametric model is chosen, then the transfer function in the set that minimizes the variance of $e(t)$ in equation (1) may be estimated in closed form as follows:

$$H(\mathrm{e}^{j2\pi f}) = \frac{S_{uy}(\mathrm{e}^{j2\pi f})}{S_{uu}(\mathrm{e}^{j2\pi f})}, \tag{2}$$

where $S_{uy}(e^{j2\pi f})$ is the cross-spectrum from $u(t)$ to $y(t)$, $S_{uu}(e^{j2\pi f})$ is the auto-spectrum of $u(t)$ and $H(e^{j2\pi f})$ is the optimal transfer function which is also known as the Wiener filter (see, e.g., Marple (1987) for a description of spectral estimation methods). Since the cross-spectrum is generally complex, the Wiener filter provides both system magnitude and phase characteristics. Additionally, the confidence in the estimated transfer function may be computed via the coherence function, $K^2(e^{j2\pi f})$:

$$K^2(e^{j2\pi f}) = \frac{|S_{uy}(e^{j2\pi f})|^2}{S_{uu}(e^{j2\pi f})S_{yy}(e^{j2\pi f})}. \tag{3}$$

The coherence function may be thought of as the squared correlation coefficient as a function of frequency. A coherence value near unity at a particular frequency indicates strong linear coupling between $u(t)$ and $y(t)$ at that frequency, whereas a coherence value near zero at the frequency reflects significant nonlinearity, nonstationary, omitted inputs and/or noise.

Nonparametric models are attractive, because they do not assume any particular mathematical structure and are relatively easy to estimate. However, in general, these models are only applicable to systems operating in open-loop conditions. This limitation is particularly significant in the context of probing the neural regulatory system, which operates in closed-loop. Consider, for example, the physiologic relationship between fluctuations in HR and ABP (see figure 2). On one hand, HR fluctuations influence ABP fluctuations through the mechanical properties of the heart and vasculature (feedforward mechanism). On the other hand, ABP fluctuations induce HR fluctuations via the neurally mediated arterial HR baroreflex (feedback mechanism). Standard nonparametric determination (i.e., with equation (2)) of the transfer functions from HR to ABP fluctuations and ABP to HR fluctuations would not result in selective representations of the feedforward mechanical and feedback neural mechanisms. Rather, each of the two estimated transfer functions would intertwine the two totally distinct physiologic mechanisms. While standard nonparametric models have nevertheless been applied to cardiovascular signals related in closed-loop, strictly speaking, these models are only appropriate when the feedback loop is experimentally opened. However, as discussed above, this type of open-loop experiment precludes study during normal physiologic conditions. It should be noted that nonparametric models may be utilized to disentangle the feedforward and feedback mechanisms as they operate in closed-loop provided that an uncorrelated reference signal is applied to the system. In this case, the optimal nonparametric filter model is determined as the ratio of the cross spectrum from the reference signal to the output and the cross spectrum from the reference signal to the input. However, application of the reference signal may likewise disrupt normal system operation.

To disentangle the feedforward and feedback mechanisms without disrupting normal operating conditions, it is necessary that (1) the feedforward and/or feedback mechanism is strictly causal (i.e., fluctuations in HR can only influence future fluctuations in ABP and/or vice versa) and (2) this causality is imposed in the model (Wellstead and Edmunds 1975). Although physical systems usually meet the first requirement, parametric models are needed to satisfy the second requirement. An extensive number of a parametric LTI models have been made available for system identification analysis (see Ljung (1999)). Below, we present two such models that have frequently been employed for probing neural cardiovascular regulation. While these models are illustrated in single-input/single-output form, we expect that extensions to multi-input/single-output form will be clear. We also describe the standard least squares techniques for identifying each model assuming that the number of parameters characterizing the investigated system (model order) is known. The challenging problem of model order selection is discussed in a subsequent section.

The autoregressive exogenous input (ARX) equation is perhaps the most widely employed parametric model in identification. The ARX model with input $u(t)$ and output $y(t)$ is given as follows:

$$y(t) = \sum_{i=1}^{m} a_i y(t-i) + \sum_{i=n_l}^{n_u} b_i u(t-i) + e(t), \tag{4}$$

where $e(t)$ is an unobserved, white noise disturbance that is uncorrelated with the input $u(t)$. The unknown coefficients $\{a_i\}$ and $\{b_i\}$ are respectively referred to as the autoregressive (AR) and moving average (MA) parameters, and the summation limits m, n_l and n_u specify the number of these parameters (model order). Note that strict causality can be imposed here by not allowing n_l to be less than 1. The transfer function characterizing the input–output relationship of the ARX model may be made evident by applying the Z-transform to equation (4):

$$Y(z) = \frac{B(z)}{1 - A(z)} U(z) + \frac{1}{1 - A(z)} E(z). \tag{5}$$

This equation indicates that the ARX transfer function is parametrized by both poles and zeros. Thus, the corresponding impulse response is built from a set of complex exponential basis functions. An ARX model can therefore represent an infinite-order impulse response with only a finite number of parameters, which is a nice feature for representing complicated neural regulatory mechanisms. Equation (5) further illustrates that the influence of the unobserved, white disturbance on the system output is colored by the ARX poles. Thus, the ARX model is able to represent LTI systems in the presence of colored noise.

While other parametric models share the above features, the enhanced popularity of the ARX model is due to the fact that it is linear in its parameters (see equation (4)). Thus, estimation of the unknown parameters by minimization of the variance of $e(t)$ may be achieved analytically via the linear least squares solution. To obtain this solution, equation (4) is rewritten in vector-product notation as follows:

$$y(t) = \phi^{\mathrm{T}}(t)\theta + e(t), \tag{6}$$

where

$$\phi^{\mathrm{T}}(t) = [y(t-1) \cdots y(t-m) \quad u(t-n_l) \cdots u(t-n_h)]$$

$$\theta^{\mathrm{T}} = \begin{bmatrix} a_1 \cdots a_m & b_{n_l} \cdots b_{n_h} \end{bmatrix}.$$

The linear least squares solution ($\hat{\theta}$) determined from N pairs of measured samples of $u(t)$ and $y(t)$ may then be given as follows:

$$\hat{\theta} = \left\{ \frac{1}{N} \sum_{t=1}^{N} \phi(t)\phi^{\mathrm{T}}(t) \right\}^{-1} \frac{1}{N} \sum_{t=1}^{N} \phi(t) y(t), \tag{7}$$

provided that the above inverse exists (i.e., the data are sufficiently informative). Importantly, the uncertainty in $\hat{\theta}$ may also be estimated (see Ljung (1999)) and mapped to approximate the uncertainty in the physically meaningful impulse response (Perrott and Cohen 1996).

A limitation of the ARX configuration is that it does not include parameters that solely account for noise coloring, as the model poles are also utilized to represent the impulse response. Thus, the number of parameters required to represent a system with an ARX model may be unnecessarily high. Among the more flexible parametric LTI models that have been made available, the generalized least squares (GLS) model (also known as the ARARX model) may be the most popular. The Z-transform of the GLS model is given as follows:

$$(1 - A(z))Y(z) = B(z)U(z) + \frac{1}{D(z)} E(z), \tag{8}$$

where the additional polynomial $D(z)$ serves to represent only the disturbance to the system output. The disadvantage of the GLS model with respect to the ARX model is that it is not linear in its parameters, and thus, parameter estimation may not be achieved in closed form. However, if $D(z)$ were known, then the model would be linear in the parameters of $A(z)$ and $B(z)$. On the other hand, if the parameters in $A(z)$ and $B(z)$ were both known, then the model would be linear in the parameters of $D(z)$. Thus, rather than conducting a full numerical search, the GLS parameters may be conveniently estimated by a back-to-back iteration between two analytic linear least squares solutions with an initial guess for the parameters in $D(z)$. (Note that this iteration is not guaranteed to converge to the global minimum.) Additionally, a measure of the uncertainty in the resulting GLS model may be computed (see Ljung (1999) and Perrott and Cohen (1996)).

Finally, we note that the assumption of a particular input–output structure by parametric models such as those above may be unsatisfying. However, as implied above, this assumption facilitates unique model determination even when limited information is available in the measured data.

3.2.5. Time-variant models. If the system to be identified is regarded as linear but time varying (LTV), then the input–output relationship is characterized according to the convolution sum of equation (1) with $h(t, i)$ replacing $h(t-i)$. The LTV system impulse response $h(t, i)$ is usually identified by (1) selecting a time window for which the data are assumed to be stationary (i.e., piece-wise stationary), (2) scaling the measured data with time shifted versions of the window and (3) estimating the LTI impulse response at each time shift so as to update the impulse response over time. While the window may be defined as a rectangular function, it is often specified as an exponential function in order to enhance the influence of the most recent dynamics on model estimation. The exponential window is characterized by a 'forgetting factor' λ (generally between 0.8 and 1), which indicates the effective width of the window. If a parametric model is employed that is linear in its parameters (e.g., ARX model), then this estimation procedure may be solved efficiently through the recursive least squares (RLS) algorithm. Inheriting the notation in equation (6), the RLS estimate at time t can be derived based on that of $t-1$ as follows:

$$\hat{\theta}(t)_{\mathrm{RLS}} = \hat{\theta}(t-1)_{\mathrm{RLS}} + K(t)(y(t) - \phi^{\mathrm{T}}(t)\hat{\theta}(t-1)), \tag{9}$$

where

$$K(t) = P(t-1)\phi(t)[\lambda I + \phi^{\mathrm{T}}(t)P(t-1)\phi(t)]^{-1}$$

$$P(t) = [I - K(t)\varphi^{\mathrm{T}}(t)]P(t-1)/\lambda.$$

The initial values $\hat{\theta}(0)$ and $P(0)$ can be estimated by utilizing *a priori* information or taken arbitrarily as 0 and ρI, respectively, where ρ is a 'large' number (see Soderstrom and Stoica (1988)). The choice of the value of the forgetting factor is often very important. A large forgetting factor (near 1) leads to good convergence properties and small variance of the parameter estimates, while a small forgetting factor enhances alertness and ability of the algorithm to track time variations of the system parameters. Note that this approach is not able to handle rapidly varying systems, which require a very small forgetting factor leading to increased sensitivity to noise. A solution for these types of systems is to expand each model parameter onto a set of time-varying basis functions (e.g., Subba Rao (1970)). However, a uniform rule does not exist in choosing the particular type of basis functions.

3.2.6. Nonlinear models. If the system to be identified is regarded as nonlinear and time invariant with finite memory, then the Volterra series may be utilized to specify the candidate

model set for characterizing the general input–output relationship. The Volterra series is an infinite sum of functionals representing multidimensional convolutions of increasing order and may therefore be thought of as a generalization of linear convolution in equation (1). The discrete-time Volterra series causally relating the input $u(t)$ to the output $y(t)$ is given as follows:

$$y(t) = k_0 + \sum_{i=0}^{p} k_1(i)u(t-i) + \sum_{i_1=0}^{p}\sum_{i_2=0}^{p} k_2(i_1, i_2)u(t-i_1)u(t-i_2) + \cdots + \mathrm{e}(t), \tag{10}$$

where the summation limits p represent the finite system memory; $\mathrm{e}(t)$ is an unobserved, stochastic process of zero mean that is uncorrelated to $u(t)$ and k_0, $k_1(t)$, $k_2(t_1, t_2), \ldots$ are the Volterra kernels which completely characterize the above system. The zeroth-order constant kernel k_0 represents the system response to zero input, whereas the first-order functional is exactly the linear convolution sum. However, the impulse response of the above system is not given by the first-order kernel $k_1(t)$ but rather is determined from components of all the kernels. The higher order kernels represent nonlinear interaction effects. While it is often difficult to obtain intuition about system behavior from these kernels, the kernels may be utilized to predict the system output for a given input. Finally, note that generalizing equation (10) to multiple inputs would also include cross term functionals that consist of different inputs within a multidimensional convolution sum.

To facilitate the estimation of the optimal system kernels in the set from the generated input–output data, the Volterra functionals may be transformed into an orthogonal set of functionals. In this way, the estimation of the kernel associated with each orthogonal functional may be performed one at a time without any confounding influence from the other functionals. The Wiener series is such a set of functionals obtained by orthogonalizing the Volterra functionals via a Gram–Schmidt procedure in which the input signal is a zero-mean Gaussian white noise. The discrete-time, causal Wiener series is specifically given as follows:

$$y(t) = \sum_{n=0}^{\infty} H_n[u(t)] + \mathrm{e}(t), \tag{11}$$

where the first three orthogonal functionals are

$$H_0[u(t)] = h_0, \qquad H_1[u(t)] = \sum_{i=0}^{p} h_1(i)u(t-i),$$

$$H_2[u(t)] = \sum_{i_1=0}^{p}\sum_{i_2=0}^{p} h_2(i_1, i_2)u(t-i_1)u(t-i_2) - \gamma \sum_{i=0}^{p} h_2(i, i);$$

h_0, $h_1(t)$, $h_2(t_1, t_2), \ldots$ are the Wiener kernels and γ is the variance of the white noise input. The Volterra kernels may be derived from the Wiener kernels and vice versa (see Marmarelis and Marmarelis (1978)). For systems including up to second-order kernels (i.e., second-order nonlinear systems), the first- and second-order Wiener and Volterra kernels are identical.

The most simple and popular approach for estimating the Wiener kernels is by way of cross correlation. To employ this approach, a zero-mean Gaussian white noise input must be applied to the investigated system. Then, the zeroth-order kernel may be computed as the mean of the resulting output and the remaining Wiener kernels may be estimated recursively starting from the first-order kernel as follows:

$$h_n(i_1, \ldots i_n) = \frac{1}{n!\lambda^n} E\left\{\left(y(t) - \sum_{m=0}^{n-1} H_m[u(t)]\right) u(t-i_1)\cdots u(t-i_n)\right\}. \tag{12}$$

In addition to the strict Gaussian white noise requirement, a further limitation of this approach is that the estimation variance of the higher order kernels is considerable, unless long data records are available.

The kernels may also be estimated according to a parametric approach (Marmarelis 1993, Watanbe and Stark 1975). That is, each kernel is represented as a linear combination of orthonormal Laguerre functions as follows:

$$h_n(i_1, \ldots, i_n) = \sum_{j_1=0}^{q} \cdots \sum_{j_n=0}^{q} c_{j_1,\ldots,j_n} L_{j_1}(i_1) \ldots L_{j_n}(i_n), \tag{13}$$

where $\{c_{j_1 \ldots j_n}\}$ are the Laguerre parameters, the summation limits q specify the number of these parameters (model order) and the jth-order Laguerre function, $L_j(t)$, is defined as

$$L_j(t) = \alpha^{(t-j)/2}(1-\alpha)^{1/2} \sum_{i=0}^{j} (-1)^i \binom{t}{i} \binom{j}{i} \alpha^{j-i}(1-\alpha)^i$$

with α establishing the decay rate of the Laguerre functions. For a fixed model order, the Laguerre parameters may be estimated from the input–output data through the linear least squares solution (substitute equation (13) into equation (11)). This parametric approach can sometimes provide a more compact representation of the system kernels and therefore reduce the estimation error variance for a given length of data record. Moreover, strict whiteness of the input is not necessary. (However, when the input deviates significantly from white noise, then the Wiener series functionals are no longer orthogonal.) A disadvantage of this approach is that it may be difficult to specify appropriate values for α and p. Note that a further reduction in the parameters needed for system representation may be achieved with nonlinear ARX models in conjunction with Laguerre functions (Chon *et al* 1997a). It should also be noted that the above approaches are typically effective in estimating only up to second- or third-order kernels.

In addition to the Volterra–Wiener series, conditional probability density functions may also be utilized to represent the input–output relationship of a general nonlinear and time-invariant system (e.g., $P(y(t)/u(t-1), \ldots, u(t-r))$ where r is the model order). The probability functions may be estimated, for example, by the nonparametric Parzen window technique (Parzen 1962). Then, an index of the estimated probability function may be computed to indicate succinctly the statistical (rather than just linear) dependence of the past values of the input on the output. One such index is the conditional entropy (e.g., $-E\{\log[P(y(t)/u(t-1), \ldots, u(t-r)]\}$), which summarizes the randomness of $y(t)$ given the r previous values of $u(t)$. Although this type of candidate model set is powerful from a theoretical point of view, in practice, nonparametric probability estimators require enormous data sets and are typically unreliable even with modest values of r. Note that parametric density estimators (e.g., Gaussian mixture models (Dempster *et al* 1977)) or heuristic procedures (Porta *et al* 1999) can alleviate this significant limitation.

3.2.7. Model order selection. To capitalize fully on the benefits afforded by parametric models, the problem of determining the number of parameters needed for system representation must be confronted. This so-called model order selection problem may be tackled by first establishing a set of candidate model orders and then determining the 'best' model order in the set.

Forming an appropriate candidate model order set is a difficult task that amounts to a trade-off between completeness of the set and computational tractability. Typically, the candidate set is established simply with models of successively increasing number of parameters (e.g.,

Table 2. Selected model order selection criteria.

Criterion	Formula	Physical meaning
A-information criterion (AIC)	$\mathrm{AIC} = \log\left(\frac{V(p,N)}{N}\right) + \frac{2p}{N}$	A metric of the difference between the actual and estimated unobserved disturbance
Final prediction error (FPE)	$\mathrm{FPE} = V(p,N)\left(1+\frac{p}{N}\right)/\left(1-\frac{p}{N}\right)$	Estimate of the expected value of the loss function that would be obtained with new data
Minimum description length (MDL)	$\mathrm{MDL} = V(p,N)\left(1+\frac{p}{N}\cdot\log N\right)$	Number of bits (information) needed to represent the estimated model parameters
Vapnik's measure (VM)	$VM = V(p,N)\left(1-\sqrt{\frac{p(1+\log(N/p))+\log N/2}{N}}\right)^{-1}$	An upper bound on the loss function that would be obtained with new data

$V(p,N)$ is the minimum loss function computed with p parameters and the N data samples available for analysis.

successively increasing values of m and n_u in equation (4)) up to a maximal model order that is believed to nest the 'true' system parametrization. However, more sophisticated, data driven approaches have also been proposed that are based on, for example, the significance of each estimated parameter of a maximal model (Perrott and Cohen 1996) or the group method of data handling (Chon and Lu 2001).

The selection of an optimal model order in the chosen set may be an equally challenging task. For example, suppose the best model order in the set is selected by minimizing the variance of the unobserved disturbance (loss function). However, the loss function is a monotonically decreasing function of the model order, and this approach would therefore result in an overly complicated model that fits the particular realization of the unobserved noise corrupting the measured data. On the other hand, this approach would prove successful if it were applied to a fresh set of data not utilized for parameter estimation, because these data would be corrupted by a different realization of unobserved noise. This cross validation approach is indeed an effective option for selecting the best model order. However, the trade-off is that not all the measured data can be utilized for parameter estimation. Thus, due to asymptotic arguments, the quality of the models to be selected from will not be as high as possible. Several strategies have been proposed to avoid overparametrization while utilizing all the data for parameter estimation (see Ljung (1999)). The most popular strategy is to minimize a theoretically derived formula or criterion, which includes a goodness-of-fit index such as the loss function and a penalty factor for model complexity (see table 2). Amongst the most widely used criteria, the final prediction error (FPE) does not satisfactorily prevent overparametrization, whereas the minimum description length (MDL) criterion is able to do so but only for large data samples (Gustafsson and Hjalmarsson 1995). However, the recently proposed Vapnik's measure (VM) based on structural risk minimization (SRM) may be more effective in model order selection than classical criteria (Cherkassky and Ma 2003). Strictly speaking, most of these criteria are only applicable to models that are identified with the linear least squares solution (e.g., ARX model). For more general models, model order selection based on achievement of a pre-defined value of the loss function normalized by the output

variance (Qi and Zhang 2001) or the more general SRM approach (Cherkassky *et al* 1999) may be considered.

3.3. Model validation

Once the best model in a candidate set has been determined from the generated data, a final step remains as to demonstrate the validity of the model for its intended purpose. For example, a linear model need only be validated in terms of representing the small signal behavior of the investigated neural regulatory mechanism around the current operating point. The most convincing approach for model validation would be to obtain an independent measure of the system dynamics (without the use of system identification) against which the estimated model may be compared. Unfortunately, such an independent measurement would require precise control of the studied inputs that would be very difficult to achieve experimentally. For example, to obtain an independent measure of an impulse response or step response (integral of the impulse response), an impulse or step change would have to be applied to appropriate point in the neural regulatory system while all other investigated inputs are held perfectly constant. A more realizable approach for model validation would involve obtaining an independent measure of the system dynamics by application of system identification to data obtained under different experimental conditions. For example, a model estimated from spontaneous beat-to-beat variability may be validated against the corresponding model estimated from data collected during precise randomized control of the considered inputs (to ensure sufficient information). Note that, in establishing either of these independent measures, closed-loop operation of the neural regulatory system would invariably be destroyed. Thus, comparisons with models estimated from different operating conditions should be made with caution.

While demonstrating the quantitative validity of models (e.g., time constants) estimated from experimental data may be difficult, other more practical, but less convincing, validation approaches may be employed. One approach is to apply the system identification method to computer simulated data and compare the resulting model estimates with the actual system dynamics responsible for generating the data. Of course, this type of theoretical validation would only be as meaningful as the extent to which the simulated data coincide with experimental data. A simple validation approach that utilizes experimental data is to illustrate that the identified model is consistent with known physiologic mechanisms. For example, since the arterial HR baroreflex is known to be a negative feedback mechanism, the estimated step response relating fluctuations in ABP to HR can be shown to reach asymptotically a value below zero. Another experimental approach that is far more powerful is to demonstrate that the estimated dynamics change appropriately in response to known alterations to the system. For example, the impulse response estimate relating fluctuations in ILV to HR, which characterizes the direct neural coupling mechanism, can be shown to diminish after pharmacological blockade of the autonomic nervous system. Finally, if the model is not supported by any of the above or alternative means, then the previous system identification steps should be modified and repeated until model validation is achieved.

4. Review of progress

Over the past two decades, numerous system identification studies for probing neural cardiovascular regulation have appeared in the literature. These studies have mostly focused on the quantitative characterization of the SA node, RSA mechanisms and the baroreflex.

In this section, we review the progress that has been made with respect to these neural regulatory mechanisms. It should be noted that we do not intend to provide an exhaustive, detailed coverage of all related literature but rather to review selected studies with the goal of enhancing our insight and fostering novel ideas for future exploration.

4.1. The sinoatrial node

The HR response of the SA node to the changes in vagal and β-sympathetic excitation (see figure 2) has been examined for many decades. The initial efforts were not based on mathematical analysis methods. For example, Penaz (1962) and Chess and Calaresu (1971) investigated the response of the SA node to sinusoidal stimulation of the vagus nerves in rabbits and cats, respectively. To assess system behavior over a wide frequency range, their approach required numerous trials to vary the frequency of the sinusoidal stimulation.

To achieve a more efficient input–output characterization of the SA node, Berger *et al* (1989b) stimulated the vagus and sympathetic nerves of dogs with Gaussian white noise bandlimited to 0.7 Hz and measured the resulting HR response. In this study, all endogenous neural influences to HR were interrupted. These investigators then employed standard nonparametric LTI analysis to show that the SA node behaved as a low-pass filter in response to either parasympathetic or β-sympathetic stimulation with the β-sympathetic filter having a much lower corner frequency than the vagal filter. They also demonstrated that the filter characteristics depended significantly on the mean level of vagal and sympathetic stimulation. Thus, the linearity approximation of the SA node could only be valid for small perturbations.

Berger *et al* (1989b) selectively stimulated one set of cardiac nerves at a time with the other set remaining inactive. However, prior experimental studies not employing system identification (Furukawa and Levy 1984, Levy 1984, Mace and Levy 1983) have shown that the SA node system behavior is dependent on the interaction between parasympathetic and β-sympathetic excitations. To examine this nonlinearity with system identification, Kawada *et al* (1996) carried out experiments in which one set of cardiac nerves was stimulated with band-limited Gaussian white noise, while the other set was excited tonically (i.e., with constant frequency). These investigators then employed standard nonparametric LTI analysis to identify the filter properties relating the white noise nerve stimulation to the HR response. They verified the previous experimental studies by showing that the gains of both the β-sympathetic and parasympathetic filters were augmented by the concomitant tonic stimulation. These investigators postulated that by virtue of this interaction, the autonomic nervous system is able to extend its dynamic range of operation.

In the above studies, the SA node system dynamics were examined by modulating the frequency of the nerve stimulation without regard to their time of arrival in the cardiac cycle. However, phase dependence of the chronotopic response to autonomic stimulation, especially in the vagal branch, has been experimentally demonstrated (Katona *et al* 1970, Levy *et al* 1969). To assess quantitatively any phase dependence, Mokrane *et al* (1995) applied beat-to-beat stimulatory pulses to the vagus nerves synchronized to the A waves of the atrial electrogram. These investigators then utilized standard nonparametric LTI analysis to identify the filter characteristics relating the nerve stimulation to the sinus rate response. They showed that the estimated filter included two components, one slow and one fast. They also demonstrated phase dependence of the SA node by reporting that the fast component was not found in the filter estimated from nonsynchronized vagal stimulation.

The findings from the above system identification studies have not only provided a solid basis for forward modeling of related processes (Chiu and Kao 2001, Pyetan and Akselrod 2003) but have also enabled the development of a noninvasive methods for selectively

quantifying parasympathetic and β-sympathetic responsiveness (see section 4.2) as well as for estimating SA node dynamic properties. With regard to the latter topic, Porta *et al* (2003) aimed to model the SA node from only noninvasively measured, spontaneous fluctuations in the RR interval (RRI, inverse of HR), systolic blood pressure (SBP) and respiration. These investigators specifically employed a causal, dual-input ARARX model with RRI as the output (Baselli *et al* 1988, Porta *et al* 2000). They then assumed that the dynamic properties of the SA node were related to the AR terms of the model. Using experimental data, these investigators demonstrated that the estimated SA node dynamics were low frequency dominant, obliterated in heart transplant patients, and altered by high-dose atropine injection. Although this measure of SA node behavior may not be specific, this work represents the first attempt to noninvasively estimate these important dynamics through system identification.

4.2. Respiratory sinus arrhythmia mechanisms

To identify the physiologic mechanisms responsible for mediating RSA, the respiratory input signal is usually measured in terms of ILV while the output signal is given as either HR or RRI. Since the ILV signal measured during spontaneous breathing is normally narrow-band, early studies of the relationship between ILV and HR relied on fixed rate breathing experiments to probe the system over a range of frequencies (Hirsch and Bishop 1981). To study this relationship more efficiently, Berger *et al* (1989a) devised a broadband breathing protocol in which the subject inspires on cue to a sequence of auditory tones spaced at random intervals in time. These investigators demonstrated that this random interval breathing protocol substantially broadens the spectral content of the ILV signal. The subsequent system identification investigations below have all employed this protocol in order to characterize the open-loop ILV to HR coupling over a broad range of frequencies.

Saul *et al* (1989, 1991) identified the transfer function from ILV to HR in humans based on standard nonparametric LTI analysis. These investigators utilized postural changes and pharmacological autonomic blockade to gain insight into the resulting transfer function estimates. They reported that the estimated RSA transfer function resembled a low-pass filter and that it included both cardiac sympathetic and parasympathetic components. The sympathetic component was low frequency dominant, whereas the parasympathetic component was characterized by high magnitude in both the low and high frequency regimes with a slight phase lead (i.e., a noncausal system in which HR alterations lead respiration).

Parametric LTI methods have also been applied to investigate the ILV to HR coupling. Yana *et al* (1993) employed a single-input, single-output MA model to couple the fluctuations in ILV to HR. Subsequently, Mullen *et al* (1997) and Triedman *et al* (1995) introduced a dual-input ARX model that also accounted for the baroreflex influence of ABP on HR. (The validity of this identification method was later supported with respect to a realistic human cardiovascular simulator (Mukkamala and Cohen 2001).) These parametric models confirmed the noncausality of the ILV to HR coupling. Importantly, Triedman *et al* (1995) observed that the ILV to HR impulse response typically included two components, a fast, positive deflection and a delayed, slower negative deflection with lower magnitude. Moreover, Mullen *et al* (1997) and Triedman *et al* (1995) demonstrated that each of these deflections was nearly obliterated after pharmacological autonomic blockade, thereby indicating that the ILV to HR coupling is indeed a neurally mediated regulatory mechanism. Based on these findings and the data from the SA node experiments of Berger *et al* (1989b) (see section 4.1), Xiao *et al* (2004) assumed that the initial, positive wave in the ILV to HR impulse response was a consequence of parasympathetic withdrawal and the slower, negative wave was a reflection of β-sympathetic withdrawal. These investigators then showed through postural changes that

the areas of the positive and negative waves can respectively provide selective quantification of parasympathetic and β-sympathetic responsiveness. This technique may improve upon HR spectral analysis, which is only able to provide selective quantification of parasympathetic responsiveness (though respiratory effort may be a confounding factor here).

In an interesting comparative study, Barbieri *et al* (1997) evaluated the ILV to HR transfer function estimated from both single-input (ILV) and dual-input (ILV and ABP) ARX models. These investigators found that the gain of the transfer function estimates (defined as its amplitude at the frequency associated with the largest coherence in the HF range of 0.15–0.5 Hz) was significantly lower using the dual-input model. This finding may be due to differences in the physiologic meaning of the two differently estimated transfer functions. That is, the transfer function estimated from the single-input model is representative of the direct neural coupling mechanism between respiration and HR as well as the interaction between ABP and HR (due to the correlation between ILV and ABP), while the transfer function identified with the dual-input model does not encompass the ABP interactions.

Besides ABP, the cardiopulmonary baroreflex control of HR may also complicate the coupling of ILV to HR. Through simulation studies, Mukkamala and Cohen (2001) showed that the ILV to HR impulse response identified with a dual-input ARX model may also be reflective of the cardiopulmonary baroreflex due to the tight correlation between ILV and RAP. Barbieri *et al* (2002) studied the ILV to RRI gain (as defined above) in humans based on a single-input ARX model at six different levels of RAP induced by lower body negative pressure, leg raise and saline infusion. They found that the gains (both in the LF range of 0.04–0.15 Hz and HF range) generally increased with RAP. However, at the highest investigated RAP level, the gains decreased, thereby indicating a Bainbridge-type of reflex at hypervolemic states. These interesting findings may suggest a nonlinear interaction between the ILV to HR coupling and the cardiopulmonary baroreflex. However, since a single-input model was employed, it may be difficult to determine if the nonlinear interactions are between these two mechanisms and/or the arterial and cardiopulmonary baroreflex systems (see section 4.3.2).

While most studies have utilized linear models to represent the ILV to HR coupling, only a couple of studies have sought to elucidate more complicated behaviors through nonlinear models. Ahmed *et al* (1986) examined the effect of controlled breathing on HR by attempting to identify a second-order nonlinear Volterra model. These investigators interpreted the second-order kernel as indicating 'a restraining force' and 'an escape-like phenomenon' in the system. However, they did not take into account the effects of ABP on HR. Chon *et al* (1996) incorporated these effects through a second-order, dual-input Volterra model in which Laguerre functions were utilized to parametrize the system kernels. These investigators reported a considerable reduction in both first-order and second-order ILV to HR kernel amplitudes after autonomic double blockade in humans (see section 4.3.2).

Finally, the ILV to HR coupling has also been assessed under a few patho-physiologic conditions. Freeman *et al* (1995) employed standard nonparametric LTI analysis to estimate the ILV to HR transfer function in patients with diabetic autonomic neuropathy. These investigators reported significant differences in the transfer function amplitude and phase between healthy controls and patients with varying degrees of autonomic dysfunction. Mukkamala *et al* (1999) also studied the ILV to HR coupling in diabetic patients, but they implemented the dual-input ARX technique of Mullen *et al* (1997) in their investigation. They found that the peak amplitude of the ILV to HR impulse response decreased with increasing severity of the disease. Moreover, they reported that this parameter was more sensitive in detecting autonomic dysfunction than both the conventional methods and HR spectral analysis. Stanley *et al* (1996, 1997) examined age effects on the ILV to HR coupling using standard nonparametric LTI analysis. They reported that the magnitude of

the estimated transfer function tended to decrease with age, and the HR response to ILV stimulation was slower in older subjects than in younger subjects. These results are consistent with prior knowledge that parasympathetic function decreases with aging. Xiao *et al* (2004) utilized the ILV to HR impulse response to assess both parasympathetic and β-sympathetic responsiveness (see above) during cardiovascular deconditioning induced by prolonged bed rest. These investigators found that both β-sympathetic and parasympathetic responsiveness were diminished in the subjects after the bed rest and that the subjects with high sympathetic responsiveness and low parasympathetic responsiveness at baseline tended to tolerate better orthostatic challenges both before and after bed rest.

4.3. The baroreflex

4.3.1. Control of sympathetic nerve activity. The arterial baroreflex control of regional sympathetic nerve activity (SNA) has been characterized in animals by identifying the coupling from fluctuations in ABP to SNA to a particular effector organ. While this coupling encompasses the baroreceptor and autonomic nervous function, it does not incorporate end organ function (see figure 2).

Ikeda *et al* (1996) studied the arterial baroreflex response of cardiac SNA to changes in carotid sinus pressure (CSP) in rabbits. These investigators experimentally opened the baroreflex loops by sectioning the vagus and aortic depressor nerves and perturbing CSP over a wide range with a binary white noise process. Using standard nonparametric LTI analysis, they found that the estimated transfer function relating CSP to the cardiac SNA behaved as a high-pass filter with a passband between 0.1 Hz and 1 Hz. Through simulation studies, these investigators concluded that these filter characteristics optimized closed-loop ABP regulation in terms of stability and quickness.

While the above investigation characterized the carotid sinus baroreflex during open-loop conditions, Kawada *et al* (1997, 2000) sought to characterize the CSP to cardiac SNA coupling as it operates in closed-loop. Rather than dealing with the difficulties involved in identifying parametric models, these investigators were able to utilize a more convenient, nonparametric LTI model by introducing a reference white noise perturbation to aortic pressure or the aortic depressor nerve in rabbits. This approach resulted in CSP variations over a wide range. Importantly, they showed that parameters of the transfer function estimated under the closed-loop conditions did not significantly differ from those identified by experimentally opening the loop.

The above system identification studies approximated the carotid sinus baroreflex control of the SNA with linear models. However, previous experimental studies have indicated that the static relationship of the ABP to SNA coupling resembles a sigmoid rather than a line (Mohrman and Heller 1997, Sato *et al* 1999). Such nonlinear threshold and saturation effects may render a linear approximation to be dependent on both input amplitude and operating point. To circumvent this problem, Sato *et al* (2003) studied the open-loop relationship from CSP to renal SNA in rats by limiting the range of CSP perturbations to be within ± 10 mm Hg in order for the linearity approximation to be more tenable. Using standard nonparametric LTI analysis, they reported that the estimated transfer function from CSP to renal SNA also possessed highpass filter characteristics. Kawada *et al* (2003) examined the effect of input amplitude on the open-loop transfer function relating CSP to cardiac SNA as identified by standard nonparametric LTI analysis. They confirmed the existence of the sigmoidal static nonlinearity by showing that the static gain as well as the slope of the transition band of the high pass transfer function estimates both decreased with increasing binary white noise input amplitude. Importantly, they also demonstrated that a model consisting of linear dynamics

followed by a static sigmoidal nonlinearity (rather than vice versa) represents a good first approximation of the characteristics of the carotid sinus baroreflex control of SNA. This result suggests that the baroreflex nonlinearity may dominate in the efferent pathway rather than at the baroreceptors.

4.3.2. Control of HR. As discussed in section 3.1.1, the arterial HR baroreflex has been the subject of many system identification studies due to its importance in neural regulation and the relative ease of measuring the ABP input signal and the HR (or RRI) output signal. (Note that the coupling from ABP to HR encompasses baroreceptor, autonomic nervous system and SA node effector organ function.) In these studies, either average ABP or SBP has been regarded as the system input. Since the variance of SBP is usually larger than average ABP, the HR baroreflex gains may be dependent on the particular input variable that is chosen. However, there is no in-depth discussion or consensus in the literature regarding the appropriateness of either variable.

The most simple method that has been employed for the identification of the arterial HR baroreflex is standard nonparametric LTI analysis of spontaneous HR and ABP fluctuations (Malliani *et al* 1991, Pagani *et al* 1988, Robbe *et al* 1987, Saul *et al* 1991). An assumption of this single-input method is that all other influences on HR variability are negligible. However, as discussed above, the RSA phenomenon is also important. Thus, the resulting arterial HR baroreflex transfer function estimates may be biased by correlated respiratory fluctuations. On the other hand, since spontaneous respiratory activity mainly resides in the HF range, the LF transfer function estimates should be less affected by respiration and more reliable than the HF estimates. Indeed, the enhanced reliability of the LF transfer function estimates has been indicated in several previous studies (de Boer *et al* 1985, Guasti *et al* 2002, Taylor and Eckberg 1996). Thus, the arterial HR baroreflex as identified in this manner is usually carried out in the LF and HF regions separately.

Standard nonparametric LTI analysis is not only convenient but has also been shown to provide a sensitive measure of arterial HR baroreflex functioning in both experimental and clinical studies. For example, using this method, Saul *et al* (1991) showed that autonomic changes induced by pharmacological blockade can be detected in the arterial HR baroreflex transfer function magnitude (for additional examples, see table 3 and the review by Lanfranchi and Somers (2002)). On the other hand, there is also considerable evidence indicating poor agreement between the results of nonparametric LTI analysis and those based on conventional methods for measuring the arterial HR baroreflex (e.g., phenylephrine administration), especially in individuals with mild or more severe cardiovascular disease (Colombo *et al* 1999, Lipman *et al* 2003, Maestri *et al* 1998, Pitzalis *et al* 1998). This is likely due to the fact that standard nonparametric LTI analysis intertwines the feedforward and feedback couplings between ABP and HR. Thus, this type of analysis may provide a sensitive but nonspecific measure of the arterial HR baroreflex.

If the feedback loop were experimentally opened (see section 4.3.1), then standard nonparametric LTI analysis may be utilized to characterize baroreflex functioning distinctly. However, as we have discussed, this approach may disrupt normal physiologic conditions. Akselrod *et al* (1985) proposed a nonparametric method to disentangle the feedback loop from spontaneous, resting fluctuations but only over a particular band of frequencies. These investigators argued that LF HR fluctuations in conscious dogs are solely due to mediation by the arterial baroreflex. Based on this assumption, they showed that the transfer function of the arterial HR baroreflex in the LF regime can be decoupled from its feedforward counterpart by using auto-spectral analysis of ABP and HR fluctuations. However, this interesting method has not been subsequently verified.

Table 3. Summary of selected system identification studies of the arterial HR baroreflex under different clinical or physiological conditions.

Condition	References	Population	Data	Method	Findings
Hypertension (HTN)	(Pagani *et al* 1988)	7 hypertensive, 7 normotensive	Spontaneous ABP and ECG	Nonparametric LTI model	↓baroreflex gain with HTN
Diabetic autonomic neuropathy (DAN)	(Mukkamala *et al* 1999)	37 control, 60 diabetic subjects	Random breathing ILV, ABP and ECG	Dual-input ARX model	Baroreflex amplitude progressively decreased with increasing severity of DAN
Syncope	Mainardi *et al* 1997)	8 subjects with episodes of vasovagal syncope	Spontaneous ABP and ECG	LTV, single-input parametric model	Inhibition of the baroreflex preceding the syncopal event
Sleep Apnea (SA)	(Belozeroff *et al* 2002)	13 patients with SA before and after continuous positive airway pressure (CPAP) therapy	Random breathing ILV, ABP and ECG	Dual-input MA model	↑baroreflex gain in compliant subjects with CPAP therapy
Aging	(Parati *et al* 1995)	8 young and 8 elder HTN patients	Spontaneous ABP and ECG	Nonparametric LTI model	↓baroreflex sensitivity with aging
Exercise training	(Iwasaki *et al* 2003)	11 healthy subjects	Spontaneous ABP and ECG	Nonparametric LTI model	↑baroreflex sensitivity after 3 mo of training, but returned to control value at 12 mo
	(Lucini *et al* 2002)	40 ischemic heart disease 29 with exercise training, 11 controls	Spontaneous ABP, ECG and ILV	Dual-input ARARX model	↑baroreflex gain (↑cardiopulmonary component) after training
Physical deconditioning	(Iwasaki *et al* 2000)	9 healthy subjects, 2-week bed rest	Spontaneous ABP and ECG	Nonparametric LTI model	↓baroreflex gain in HF region
	(Xiao *et al* 2004)	29 healthy subjects, 16-day bed rest	Random breathing ILV, ABP and ECG	Dual-input ARX model	↓baroreflex gain after bed rest

Baselli *et al* (1988) were the first to employ parametric LTI models that impose causality and therefore permit the distinct and comprehensive characterization of the arterial HR baroreflex as it operates during normal closed-loop conditions. These investigators specifically utilized a dual-input ARARX model to represent the relationship between spontaneous fluctuations in RRI, SBP and ILV (Baselli *et al* 1988, 2001, Porta *et al* 2000). Mullen *et al* (1997), Patton *et al* (1996) and Triedman *et al* (1995) followed this work by proposing dual-input ARX models to study the interactions between HR, ABP and ILV fluctuations obtained

during random interval breathing. More recently, Faes *et al* (2004) developed a causal version of the coherence function from fluctuations in SBP to RRI based on a single-input ARX model.

Several studies have sought to compare the arterial HR baroreflex as identified from parametric and nonparametric models. Barbieri *et al* (2001), Faes *et al* (2004) and Porta *et al* (2000) showed that the arterial HR baroreflex gain derived from standard nonparametric LTI analysis is always larger than that determined using parametric models. One plausible explanation to account for this difference is that the buffering of the SBP variability by the feedforward mechanical effect of HR on SBP is attributed to the SBP to HR feedback coupling by the nonparametric model. Thus, as Barbieri *et al* (2001) states, there is an apparently larger change in HR per a unit change in SBP. In contrast, only one previous study has attempted to compare the arterial HR baroreflex as identified with parametric models to the conventional baroreflex measurement methods. In this important study, Patton *et al* (1996) reported that the maximal value of the SBP to RRI impulse response and the one-beat step response identified by a dual-input ARX model correlates with the gain value derived by the classical method involving the injection of vasoactive agents.

In identifying the arterial HR baroreflex with parametric models, some investigators have neglected respiration in the analysis (e.g., Nollo *et al* (2001) and Turjanmaa *et al* (1990)), while others have included spontaneous respiration (e.g., Baselli *et al* (1988) and Porta *et al* (2000)) or random-interval respiration as a second input (e.g., Mullen *et al* (1997), Patton *et al* (1996) and Triedman *et al* (1995)). A couple of studies have compared these approaches in terms of estimating the arterial HR baroreflex mechanism. O'Leary *et al* (1999) employed the identification method of Patton *et al* (1996) to compare the arterial HR baroreflex estimated during spontaneous and random interval breathing. These investigators found no significant difference in the maximum values of the impulse response between SBP and RRI determined from the two types of breathing patterns. This important study suggests that spontaneous breathing may excite enough frequency components in the relevant signals to enable accurate estimation of the peak value of the impulse response. Barbieri *et al* (1997) compared single-input (SBP) and dual-input (SBP and ILV) ARX models in terms of characterizing the arterial HR baroreflex during random interval breathing. Interestingly, they reported that the LF baroreflex gain was approximately the same whether the ILV signal was utilized in the model or not.

While the above studies have assumed stationarity, only a few recent studies have employed TV models to characterize the arterial HR baroreflex during transient events. Barbieri *et al* (2001), Di Virgilio *et al* (1997) and Mainardi *et al* (1997) developed single-input TV models coupling the fluctuation in SBP to RRI in which the model parameters were updated by each cardiac beat using the RLS algorithm. These investigators employed the TV models to study changes in arterial HR baroreflex functioning during physical exercise as well as vasovagal syncope (table 3). Significantly, their preliminary results indicate that the arterial HR baroreflex gain is diminished just prior to the syncopal event, which is consistent with current beliefs concerning the mechanisms responsible for vasovagal syncope.

Similarly, there have only been a few system identification studies addressing the nonlinearity of the arterial HR baroreflex. Barbieri *et al* (2002) showed that the arterial HR baroreflex gain estimated with a single-input parametric LTI model decreases with RAP. These results may suggest a nonlinear interaction between the arterial and cardiopulmonary baroreflex mechanisms (see section 4.2). Chon *et al* (1996) developed a second-order nonlinear Volterra model, which accounted for the influence of both fluctuations in ABP and ILV on HR. These investigators reported that a pure linear model accounted for approximately 67% of the variance in HR, while the second-order nonlinear model accounted for only an additional 13%. According to spectral analysis, they showed that the nonlinear contribution of the

HR variability was concentrated at frequencies below 0.05 Hz. To assess potential higher order nonlinearities, Chon *et al* (1997b) found that a third-order nonlinear model identified by neural network analysis further accounted for HR variability, whereas a fourth-order nonlinear model did not. Nollo *et al* (2002) studied the causal coupling from SBP to RRI based on cross-conditional entropy corrected for short data samples (Porta *et al* 1999). Using this index in conjunction with a surrogate data approach, these investigators reported that the arterial HR baroreflex feedback regulation was damaged after acute myocardial infarction (AMI) and nonlinear mechanisms may be more important in elderly subjects and post-AMI patients than in healthy young subjects.

While the above system identification methods may have their respective limitations, their usefulness and promise for the evaluation of arterial HR baroreflex functioning have been demonstrated in many studies. Table 3 presents a summary of selected system identification studies of the arterial HR baroreflex under different clinical or physiological conditions. Briefly, it has been shown that pathological conditions such as HTN, diabetes and syncope are associated with reduced baroreflex control; physical or physiological deconditioning (aging, prolonged bed rest) impairs the baroreflex gain; and short-term exercise training may enhance baroreflex sensitivity.

4.3.3. Control of TPR. The arterial TPR baroreflex couples fluctuations in ABP to TPR, while the cardiopulmonary TPR baroreflex relates fluctuations in RAP to TPR. There have been very few system identification studies of these two important neural regulatory mechanisms due to the difficulties in determining beat-to-beat TPR fluctuations and the invasiveness needed to measure RAP. To circumvent these problems, Mukkamala *et al* (2003) proposed a potentially noninvasive identification method that analyzes beat-to-beat measurements of ABP, CO and SV. Their method is based on the concept that the dynamic relationships between fluctuations in the measured signals indirectly reflect the fluctuations in TPR that are induced by the baroreflex mechanisms. These investigators specifically formulated physiologic models to show that the static gains characterizing each TPR baroreflex mechanism may be computed based on the identified impulse responses from CO to ABP and SV to ABP. They then corroborated this method in a cardiovascular simulator study. Based on this work, Aljuri and Cohen (2004) and Aljuri *et al* (2004) developed invasive methods to identify the static gains as well as the impulse responses of each TPR baroreflex mechanism. These investigators ensured sufficiently informative data by decorrelating the inputs (ABP and RAP) via the application of two independent excitation sources: random pacing of the heart and random inflation/deflation of a balloon catheter in the inferior vena cava. However, the above TPR baroreflex identification methods are yet to be fully validated.

5. Discussion and conclusions

Short-term, beat-to-beat cardiovascular variability reflects the interplay between naturally occurring physiologic perturbations to the circulation and the dynamic, compensatory response of neurally mediated regulatory mechanisms. This physiologic information may be deciphered from the subtle, beat-to-beat variations by use of modern digital signal processing techniques. While single signal analysis techniques (e.g., power spectral analysis) may be employed to quantify the variability itself, the multi-signal approach of system identification provides a powerful means to characterize the dynamic input–output properties of the neural regulatory mechanisms responsible for generating the variability.

Over the past two decades, many system identification studies for quantitatively probing neural cardiovascular regulation have appeared in the literature. Some of these studies have involved the invasive application of randomized perturbations so as to ensure that the measured beat-to-beat variability is sufficiently informative for subsequent estimation of system dynamics. Like conventional probing methods, these particular studies effectively opened the feedback loop. In contrast to the conventional methods, the use of system identification permitted, for the first time, a comprehensive dynamical representation of neural regulatory mechanisms including the SA node and the carotid sinus baroreflex control of SNA. However, an advantage of system identification is that it may also be applied to the neural regulatory system operating under normal feedback conditions. Indeed, many of the studies reported in the literature have employed system identification to study normal closed-loop neural regulation. For the most part, these studies have involved the analysis of easily measured ABP and HR in order to characterize quantitatively the arterial HR baroreflex. Although many different system identification methods have been developed and employed to elucidate the dynamics of this important mechanism, there have been very few studies comparing the relative effectiveness of each method.

While it would be most convenient to estimate the arterial HR baroreflex from only naturally occurring fluctuations, it is yet to be shown conclusively that such spontaneous variability is sufficiently informative. Thus, to identify this feedback mechanism, we currently support the use of random interval breathing, which enhances the information content in the measured variability while preserving closed-loop operation. With this broadband excitation approach, we believe that it is imperative that both ABP and easily measured ILV are simultaneously considered as inputs to HR in order to prevent estimation bias resulting from the correlation between ILV and ABP. (We would also like to point out here that other correlated inputs whose contributions to HR are lumped into the unobserved disturbance can likewise bias the estimate.) Moreover, in this way, a characterization of the direct neural coupling mechanism involved in RSA may also be obtained. We also stress the use of parametric models here to impose causality and therefore disentangle the feedback baroreflex mechanism from the feedforward mechanical coupling from HR to ABP. Finally, at least at this point, we believe that linear models may be adequate for representing the small signal behavior of the arterial HR baroreflex, as they have been shown to be effective in discriminating disease. However, we caution that it is possible that the linear models may be measuring shifts in operating point in addition to, or in lieu of, actual disease-induced changes in baroreflex functioning.

Up to now, very few studies have attempted to characterize the complex, nonlinear behavior of neural regulatory mechanisms. Thus, the precise nature of the nonlinear beat-to-beat couplings and the validity of the commonly used linearity approximation remain to be demonstrated conclusively. Likewise, there is a paucity of studies addressing the nonstationarity aspects of neural regulatory mechanisms. Thus, the manner in which neural regulatory functioning is altered during transient events such as postural changes remains poorly understood. We therefore advocate that future system identification studies of (especially the previously investigated) neural regulatory mechanisms employ nonlinear and/or time-varying techniques. Note that we have summarized these more sophisticated techniques in this review, partly to encourage their implementation in future research efforts.

We also feel that it is important that future system identification studies focus on demonstrating the validity of the estimated dynamics. We acknowledge however that such validation studies may be especially challenging if, for example, neural regulatory functioning is significantly altered from open-loop to closed-loop conditions. Finally, we believe that future system identification studies that aim to elucidate the dynamical properties of other

less understood neural regulatory mechanisms will be most beneficial. For example, very little is known about the system dynamics governing the control of TPR and VC or the cardiopulmonary baroreflex. The main challenge here is to be able to measure and/or derive the relevant signals involved.

Indeed, although many studies concerning the use of system identification for probing neural cardiovascular regulation have already been reported in the literature, there remains a strong need for future investigations of this type. We expect that future system identification studies will not only lead to the elucidation of the currently unknown dynamical properties of neural regulatory and other physiologically mediated mechanisms but also to powerful clinical tools for patient monitoring and diagnosis. It is our hope that this topical review has been both didactic and uniformly representative of the literature such that it facilitates the undertaking of such future work by researchers that are both new to and experienced in the system identification method.

Acknowledgment

The authors would like to thank Professor Roger G Mark for his encouragement in completing this manuscript.

References

Ahmed A K, Fakhouri S Y, Harness J B and Mearns A J 1986 Modelling of the control of heart rate by breathing using a kernel method *J. Theor. Biol.* **119** 67–79

Akselrod S, Gordon D, Madwed J B, Snidman N C, Shannon D C and Cohen R J 1985 Hemodynamic regulation: investigation by spectral analysis *Am. J. Physiol.* **249** H867–75

Akselrod S, Gordon D, Ubel F A, Shannon D C, Berger A C and Cohen R J 1981 Power spectrum analysis of heart rate fluctuation: a quantitative probe of beat-to-beat cardiovascular control *Science* **213** 220–2

Aljuri N and Cohen R J 2004 Theoretical considerations in the dynamic closed-loop baroreflex and autoregulatory control of total peripheral resistance *Am. J. Physiol. Heart. Circ. Physiol.* **287** H2252–73

Aljuri N, Marini R and Cohen R J 2004 Test of dynamic closed-loop baroreflex and autoregulatory control of total peripheral resistance in the intact and conscious sheep *Am. J. Physiol. Heart. Circ. Physiol.* **287** H2274–86

Baan J, van der Velde E T, de Bruin H G, Smeenk G J, Koops J, van Dijk A D, Temmerman D, Senden J and Buis B 1984 Continuous measurement of left ventricular volume in animals and humans by conductance catheter *Circulation* **70** 812–23

Barbieri R, Bianchi A M, Triedman J K, Mainardi L T, Cerutti S and Saul J P 1997 Model dependency of multivariate autoregressive spectral analysis *IEEE Eng. Med. Biol. Mag.* **16** 74–85

Barbieri R, Parati G and Saul J P 2001 Closed versus open-loop assessment of heart rate baroreflex *IEEE Eng. Med. Biol. Mag.* **20** 33–42

Barbieri R, Triedman J K and Saul J P 2002 Heart rate control and mechanical cardiopulmonary coupling to assess central volume: a systems analysis *Am. J. Physiol. Regul. Integr. Comp. Physiol.* **283** R1210–20

Baselli G, Caiani E, Porta A, Montano N, Signorini M G and Cerutti S 2002 Biomedical signal processing and modeling in cardiovascular systems *Crit. Rev. Biomed. Eng.* **30** 55–84

Baselli G, Cerutti S, Civardi S, Liberati D, Lombardi F, Malliani A and Pagani M 1986 Spectral and cross-spectral analysis of heart rate and arterial blood pressure variability signals *Comput. Biomed. Res.* **19** 520–34

Baselli G, Cerutti S, Civardi S, Malliani A and Pagani M 1988 Cardiovascular variability signals: towards the identification of a closed-loop model of the neural control mechanisms *IEEE Trans. Biomed. Eng.* **35** 1033–46

Baselli G, Porta A, Cerutti S, Caiani E G, Lucini D and Pagani M 2001 RR-arterial pressure variability relationships *Auton. Neurosci.* **90** 57–65

Belozeroff V, Berry R B, Sassoon C S and Khoo M C 2002 Effects of CPAP therapy on cardiovascular variability in obstructive sleep apnea: a closed-loop analysis *Am. J. Physiol. Heart Circ. Physiol.* **282** H110–21

Berger R D, Akselrod S, Gordon D and Cohen R J 1986 An efficient algorithm for spectral analysis of heart rate variability *IEEE Trans. Biomed. Eng.* **33** 900–4

Berger R D, Saul J P and Cohen R J 1989a Assessment of autonomic response by broad-band respiration *IEEE Trans. Biomed. Eng.* **36** 1061–5

Berger R D, Saul J P and Cohen R J 1989b Transfer function analysis of autonomic regulation: I. Canine atrial rate response *Am. J. Physiol.* **256** H142–52

Bertinieri G, Di Rienzo M, Cavallazzi A, Ferrari A U, Pedotti A and Mancia G 1988 Evaluation of baroreceptor reflex by blood pressure monitoring in unanesthetized cats *Am. J. Physiol.* **254** H377–83

Bourgeois M J, Gilbert B K, Donald D E and Wood E H 1974 Characteristics of aortic diastolic pressure decay with application to the continuous monitoring of changes in peripheral vascular resistance *Circ. Res.* **35** 56–66

Buckey J C, Lane L D Jr, Levine B D, Watenpaugh D E, Wright S J, Moore W E, Gaffney F A and Blomqvist C G 1996 Orthostatic intolerance after spaceflight *J. Appl. Physiol.* **81** 7–18

Cherkassky V and Ma Y 2003 Comparison of model selection for regression *Neural Comput.* **15** 1691–714

Cherkassky V, Shao X H, Mulier F M and Vapnik V N 1999 Model complexity control for regression using VC generalization bounds *IEEE Trans. Neural Netw.* **10** 1075–89

Chess G F and Calaresu F R 1971 Frequency response model of vagal control of heart rate in the cat *Am. J. Physiol.* **220** 554–7

Chiu H W and Kao T 2001 A mathematical model for autonomic control of heart rate variation *IEEE Eng. Med. Biol. Mag.* **20** 69–76

Chon K H, Cohen R J and Holstein-Rathlou N H 1997a Compact and accurate linear and nonlinear autoregressive moving average model parameter estimation using laguerre functions *Ann. Biomed. Eng.* **25** 731–8

Chon K H and Lu S 2001 A new algorithm for autoregression moving average model parameter estimation using group method of data handling *Ann. Biomed. Eng.* **29** 92–8

Chon K H, Mukkamala R, Toska K, Mullen T J, Armoundas A A and Cohen R J 1997b Linear and nonlinear system identification of autonomic heart-rate modulation *IEEE Eng. Med. Biol. Mag.* **16** 96–105

Chon K H, Mullen T J and Cohen R J 1996 A dual-input nonlinear system analysis of autonomic modulation of heart rate *IEEE Trans. Biomed. Eng.* **43** 530–44

Colombo R, Mazzuero G, Spinatonda G, Lanfranchi P, Giannuzzi P, Ponikowski P, Coats A J and Minuco G 1999 Comparison between spectral analysis and the phenylephrine method for the assessment of baroreflex sensitivity in chronic heart failure *Clin. Sci. (Lond)* **97** 503–13

Cooley J W and Tukey J W 1965 An algorithm for the machine calculation of complex Fourier series *Math. Comput.* **19** 297–301

de Boer R W, Karemaker J M and Strackee J 1985 Relationships between short-term blood-pressure fluctuations and heart-rate variability in resting subjects. II: a simple model *Med. Biol. Eng. Comput.* **23** 359–64

Dempster A P, Laird N M and Rubin D B 1977 Maximum likelihood from incomplete data via em algorithm *J. R. Stat. Soc. Ser. B-Methodol.* **39** 1–38

Desai T H, Collins J C, Snell M and Mosqueda-Garcia R 1997 Modeling of arterial and cardiopulmonary baroreflex control of heart rate *Am. J. Physiol.* **272** H2343–52

Di Virgilio V, Barbieri R, Mainardi L, Strano S and Cerutti S 1997 A multivariate time-variant AR method for the analysis of heart rate and arterial blood pressure *Med. Eng. Phys.* **19** 109–24

Ellis R M, Franklin D L and Rushmer R F 1956 Left ventricular dimensions recorded by sonocardiometry *Circ. Res.* **4** 684–8

Eriksen M and Walloe L 1990 Improved method for cardiac output determination in man using ultrasound Doppler technique *Med. Biol. Eng. Comput.* **28** 555–60

Ewing D J, Campbell I W and Clarke B F 1976 Mortality in diabetic autonomic neuropathy *Lancet* **1** 601–3

Faes L, Porta A, Cucino R, Cerutti S, Antolini R and Nollo G 2004 Causal transfer function analysis to describe closed loop interactions between cardiovascular and cardiorespiratory variability signals *Biol. Cybern.* **90** 390–9

Freeman R, Cohen R J and Saul J P 1995 Transfer function analysis of respiratory sinus arrhythmia: a measure of autonomic function in diabetic neuropathy *Muscle Nerve* **18** 74–84

Furukawa Y and Levy M N 1984 Temporal changes in he sympathetic-parasympathetic interactions that occur in the perfused canine atrium *Circ. Res.* **55** 835–41

Goldstein D S, Robertson D, Esler M, Straus S E and Eisenhofer G 2002 Dysautonomias: clinical disorders of the autonomic nervous system *Ann. Int. Med.* **137** 753–63

Guasti L *et al* 2002 Hypertension-related hypoalgesia, autonomic function and spontaneous baroreflex sensitivity *Auton Neurosci.* **99** 127–33

Gustafsson F and Hjalmarsson H 1995 Twenty-one ML estimators for model selection *Automatica* **31** 1377–92

Guyton A C and Hall J E 1996 *Textbook of Medical Physiology* (Philadelphia: WB Saunders)

Hales S 1733 *Statical Essays: Concerning Haemastaticks; or, an Account of Some Hydraulick and Hydrostatical Experiments Made on the Blood and Blood-Vessels of Animals* (London: W. Innys and R. Manby)

Hasser E M and Moffitt J A 2001 Regulation of sympathetic nervous system function after cardiovascular deconditioning *Ann. NY Acad. Sci.* **940** 454–68

Hirsch J A and Bishop B 1981 Respiratory sinus arrhythmia in humans: how breathing pattern modulates heart rate *Am. J. Physiol.* **241** H620–9

Hyndman B W, Kitney R I and Sayers B M 1971 Spontaneous rhythms in physiological control systems *Nature* **233** 339–41

Ikeda Y, Kawada T, Sugimachi M, Kawaguchi O, Shishido T, Sato T, Miyano H, Matsuura W, Alexander J Jr and Sunagawa K 1996 Neural arc of baroreflex optimizes dynamic pressure regulation in achieving both stability and quickness *Am. J. Physiol.* **271** H882–90

Imholz B P, Wieling W, van Montfrans G A and Wesseling K H 1998 Fifteen years experience with finger arterial pressure monitoring: assessment of the technology *Cardiovasc. Res.* **38** 605–16

Iwasaki K, Zhang R, Zuckerman J H and Levine B D 2003 Dose-response relationship of the cardiovascular adaptation to endurance training in healthy adults: how much training for what benefit? *J. Appl. Physiol.* **95** 1575–83

Iwasaki K I, Zhang R, Zuckerman J H, Pawelczyk J A and Levine B D 2000 Effect of head-down-tilt bed rest and hypovolemia on dynamic regulation of heart rate and blood pressure *Am. J. Physiol. Regul. Integr. Comp. Physiol.* **279** R2189–99

Jermendy G 2003 Clinical consequences of cardiovascular autonomic neuropathy in diabetic patients *Acta Diabetol.* **40** S370–4

Katona P G, Poitras J W, Barnett G O and Terry B S 1970 Cardiac vagal efferent activity and heart period in the carotid sinus reflex *Am. J. Physiol.* **218** 1030–7

Kawada T, Ikeda Y, Sugimachi M, Shishido T, Kawaguchi O, Yamazaki T, Alexander J and Sunagawa K Jr 1996 Bidirectional augmentation of heart rate regulation by autonomic nervous system in rabbits *Am. J. Physiol.* **271** H288–95

Kawada T, Sato T, Inagaki M, Shishido T, Tatewaki T, Yanagiya Y, Zheng C, Sugimachi M and Sunagawa K 2000 Closed-loop identification of carotid sinus baroreflex transfer characteristics using electrical stimulation *Japan. J. Physiol.* **50** 371–80

Kawada T, Sugimachi M, Sato T, Miyano H, Shishido T, Miyashita H, Yoshimura R, Takaki H, Alexander J Jr and Sunagawa K 1997 Closed-loop identification of carotid sinus baroreflex open-loop transfer characteristics in rabbits *Am. J. Physiol.* **273** H1024–31

Kawada T, Yanagiya Y, Uemura K, Miyamoto T, Zheng C, Li M, Sugimachi M and Sunagawa K 2003 Input-size dependence of the baroreflex neural arc transfer characteristics *Am. J. Physiol. Heart Circ. Physiol.* **284** H404–15

Kenner T 1988 Arterial blood pressure and its measurement *Basic Res. Cardiol.* **83** 107–21

Kitney R I 1975 Entrainment of the human RR interval by thermal stimuli *J. Physiol. Lond.* **252** 37P–38P

Kleiger R E, Miller J P, Bigger J T Jr and Moss A J 1987 Decreased heart rate variability and its association with increased mortality after acute myocardial infarction *Am. J. Cardiol.* **59** 256–62

Lanfranchi P A and Somers V K 2002 Arterial baroreflex function and cardiovascular variability: interactions and implications *Am. J. Physiol. Regul. Integr. Comp. Physiol.* **283** R815–26

Levison W H, Barnett G O and Jackson W D 1966 Nonlinear analysis of the baroreceptor reflex system *Circ. Res.* **18** 673–82

Levy M N 1984 Cardiac sympathetic-parasympathetic interactions *Fed. Proc.* **43** 2598–602

Levy M N, Martin P J, Lano T and Zieske H 1969 Paradoxical effect of vagus nerve stimulation on heart rate in dogs *Circ. Res.* **25** 303–14

Lipman R D, Salisbury J K and Taylor J A 2003 Spontaneous indices are inconsistent with arterial baroreflex gain *Hypertension* **42** 481–7

Ljung L 1999 *System Identification, Theory for the User* (Upper Saddle River, NJ: Prentice Hall)

Lucini D, Milani R V, Costantino G, Lavie C J, Porta A and Pagani M 2002 Effects of cardiac rehabilitation and exercise training on autonomic regulation in patients with coronary artery disease *Am. Heart J.* **143** 977–83

Mace S E and Levy M N 1983 Autonomic nervous control of heart rate: sympathetic-parasympathetic interactions and age related differences *Cardiovasc. Res.* **17** 547–52

Maestri R, Pinna G D, Mortara A, La Rovere M T and Tavazzi L 1998 Assessing baroreflex sensitivity in post-myocardial infarction patients: comparison of spectral and phenylephrine techniques *J. Am. Coll. Cardiol.* **31** 344–51

Mainardi L T, Bianchi A M and Cerutti S 2002 Time-frequency and time-varying analysis for assessing the dynamic responses of cardiovascular control *Crit. Rev. Biomed. Eng.* **30** 175–217

Mainardi L T, Bianchi A M, Furlan R, Piazza S, Barbieri R, di Virgilio V, Malliani A and Cerutti S 1997 Multivariate time-variant identification of cardiovascular variability signals: a beat-to-beat spectral parameter estimation in vasovagal syncope *IEEE Trans. Biomed. Eng.* **44** 978–89

Malik M and Committee 1996 Heart rate variability: standards of measurement, physiological interpretation and clinical use. Task Force of the European Society of Cardiology and the North American Society of Pacing and Electrophysiology *Circulation* **93** 1043–65

Malliani A, Pagani M, Lombardi F and Cerutti S 1991 Cardiovascular neural regulation explored in the frequency domain *Circulation* **84** 482–92

Mancia G and Mark A L 1983 Arterial baroreflexes in humans *Handbook of Physiology. The Cardiovascular System, Peripheral Circulation, Organ Blood Flow* vol III (Bethesda, MD: American Physiological Society) pp 755–93

Mansier P, Clairambault J, Charlotte N, Medigue C, Vermeiren C, LePape G, Carre F, Gounaropoulou A and Swynghedauw B 1996 Linear and non-linear analyses of heart rate variability: a minireview *Cardiovasc. Res.* **31** 371–9

Mark A L 1995 Sympathetic dysregulation in heart failure: mechanisms and therapy *Clin. Cardiol.* **18** I3–8

Marmarelis P Z and Marmarelis V Z 1978 *Analysis of Physiological Systems, the White-Noise Approach* (New York, NY: Plenum)

Marmarelis V Z 1993 Identification of nonlinear biological systems using Laguerre expansions of kernels *Ann. Biomed. Eng.* **21** 573–89

Marple S L Jr 1987 *Digital Spectral Analysis with Applications* (Englewood Cliffs, NJ: Prentice-Hall)

Mead J and Gaensler E A 1959 Esophageal and pleural pressures in man, upright and supine *J. Appl. Physiol.* **14** 81–3

Miyakawa K, Polosa C and Koepchen H P (ed) 1984 *Mechanisms of Blood Pressure Waves* (Berlin: Springer)

Mohrman D E and Heller L J 1997 *Cardiovascular Physiology* (New York: McGraw-Hill)

Mokrane A, LeBlanc A R and Nadeau R 1995 Transfer function analysis of vagal control of heart rate during synchronized vagal stimulation *Am. J. Physiol.* **269** H1931–40

Moreira E D, Ida F, Oliveira V L and Krieger E M 1992 Early depression of the baroreceptor sensitivity during onset of hypertension *Hypertension* **19** II198–201

Mukkamala R and Cohen R J 2001 A forward model-based validation of cardiovascular system identification *Am. J. Physiol. Heart Circ. Physiol.* **281** H2714–30

Mukkamala R, Mathias J M, Mullen T J, Cohen R J and Freeman R 1999 System identification of closed-loop cardiovascular control mechanisms: diabetic autonomic neuropathy *Am. J. Physiol.* **276** R905–12

Mukkamala R, Toska K and Cohen R J 2003 Noninvasive identification of the total peripheral resistance baroreflex *Am. J. Physiol. Heart Circ. Physiol.* **284** H947–59

Mullen T J, Appel M L, Mukkamala R, Mathias J M and Cohen R J 1997 System identification of closed-loop cardiovascular control: effects of posture and autonomic blockade *Am. J. Physiol.* **272** H448–61

Nollo G, Faes L, Porta A, Pellegrini B, Ravelli F, Del Greco M, Disertori M and Antolini R 2002 Evidence of unbalanced regulatory mechanism of heart rate and systolic pressure after acute myocardial infarction *Am. J. Physiol. Heart Circ. Physiol.* **283** H1200–7

Nollo G, Porta A, Faes L, Del Greco M, Disertori M and Ravelli F 2001 Causal linear parametric model for baroreflex gain assessment in patients with recent myocardial infarction *Am. J. Physiol. Heart Circ. Physiol.* **280** H1830–9

O'Leary D D, Lin D C and Hughson R L 1999 Determination of baroreflex gain using auto-regressive moving-average analysis during spontaneous breathing *Clin. Physiol.* **19** 369–77

Pagani M, Somers V, Furlan R, Dell'Orto S, Conway J, Baselli G, Cerutti S, Sleight P and Malliani A 1988 Changes in autonomic regulation induced by physical training in mild hypertension *Hypertension* **12** 600–10

Panerai R B 1998 Assessment of cerebral pressure autoregulation in humans–a review of measurement methods *Physiol. Meas.* **19** 305–38

Parati G, Frattola A, Di Rienzo M, Castiglioni P, Pedotti A and Mancia G 1995 Effects of aging on 24-h dynamic baroreceptor control of heart rate in ambulant subjects *Am. J. Physiol.* **268** H1606–12

Parzen E 1962 On estimation of a probability density and mode *Ann. Math. Stat.* **33** 1065–76

Patton D J, Triedman J K, Perrott M H, Vidian A A and Saul J P 1996 Baroreflex gain: characterization using autoregressive moving average analysis *Am. J. Physiol.* **270** H1240–9

Pawelczyk J A and Raven P B 1989 Reductions in central venous pressure improve carotid baroreflex responses in conscious men *Am. J. Physiol.* **257** H1389–95

Penaz J 1962 Frequency response of the cardiac chronotropic action of the vagus in the rabbit *Arch. Int. Physiol. Biochem.* **70** 636–50

Perrott M H and Cohen R J 1996 An efficient approach to ARMA modeling of biological systems with multiple inputs and delays *IEEE Trans. Biomed. Eng.* **43** 1–14

Pitzalis M V, Mastropasqua F, Passantino A, Massari F, Ligurgo L, Forleo C, Balducci C, Lombardi F and Rizzon P 1998 Comparison between noninvasive indices of baroreceptor sensitivity and the phenylephrine method in post-myocardial infarction patients *Circulation* **97** 1362–7

Pomeranz B *et al* 1985 Assessment of autonomic function in humans by heart rate spectral analysis *Am. J. Physiol.* **248** H151–3

Porta A, Baselli G, Lombardi F, Montano N, Malliani A and Cerutti S 1999 Conditional entropy approach for the evaluation of the coupling strength *Biol. Cybern.* **81** 119–29

Porta A, Baselli G, Rimoldi O, Malliani A and Pagani M 2000 Assessing baroreflex gain from spontaneous variability in conscious dogs: role of causality and respiration *Am. J. Physiol. Heart Circ. Physiol.* **279** H2558–67

Porta A, Montano N, Pagani M, Malliani A, Baselli G, Somers V K and van de Borne P 2003 Non-invasive model-based estimation of the sinus node dynamic properties from spontaneous cardiovascular variability series *Med. Biol. Eng. Comput.* **41** 52–61

Pyetan E and Akselrod S 2003 Do the high-frequency indexes of HRV provide a faithful assessment of cardiac vagal tone? A critical theoretical evaluation *IEEE Trans. Biomed. Eng.* **50** 777–83

Qi M and Zhang G P 2001 An investigation of model selection criteria for neural network time series forecasting *Eur. J. Oper. Res.* **132** 666–80

Raymundo H, Scher A M, O'Leary D S and Sampson P D 1989 Cardiovascular control by arterial and cardiopulmonary baroreceptors in awake dogs with atrioventricular block *Am. J. Physiol.* **257** H2048–58

Robbe H W, Mulder L J, Ruddel H, Langewitz W A, Veldman J B and Mulder G 1987 Assessment of baroreceptor reflex sensitivity by means of spectral analysis *Hypertension* **10** 538–43

Sato T, Kawada T, Inagaki M, Shishido T, Sugimachi M and Sunagawa K 2003 Dynamics of sympathetic baroreflex control of arterial pressure in rats *Am. J. Physiol. Regul. Integr. Comp. Physiol.* **285** R262–70

Sato T, Kawada T, Inagaki M, Shishido T, Takaki H, Sugimachi M and Sunagawa K 1999 New analytic framework for understanding sympathetic baroreflex control of arterial pressure *Am. J. Physiol.* **276** H2251–61

Saul J P, Berger R D, Albrecht P, Stein S P, Chen M H and Cohen R J 1991 Transfer function analysis of the circulation: unique insights into cardiovascular regulation *Am. J. Physiol.* **261** H1231–45

Saul J P, Berger R D, Chen M H and Cohen R J 1989 Transfer function analysis of autonomic regulation. II. Respiratory sinus arrhythmia *Am. J. Physiol.* **256** H153–61

Saul J P and Cohen R J 1994 Respiratory sinus arrhythmia *Vagal Control of the Heart: Experimental Basis and Clinical Implications* ed M N Levy and P J Schwartz (Armonk, NY: Futura Publishing Co. Inc.) pp 511–33

Sayers B M 1973 Analysis of heart rate variability *Ergonomics* **16** 17–32

Senzaki H, Chen C H and Kass D A 1996 Single-beat estimation of end-systolic pressure-volume relation in humans. A new method with the potential for noninvasive application *Circulation* **94** 2497–506

Soderstrom T and Stoica P 1988 *System Identification* (Englewood Cliffs, NJ: Prentice Hall)

Stanley G, Verotta D, Craft N, Siegel R A and Schwartz J B 1996 Age and autonomic effects on interrelationships between lung volume and heart rate *Am. J. Physiol.* **270** H1833–40

Stanley G, Verotta D, Craft N, Siegel R A and Schwartz J B 1997 Age effects on interrelationships between lung volume and heart rate during standing *Am. J. Physiol.* **273** H2128–34

Subba Rao T 1970 The fitting of nonstationary time-series models with time-dependent parameters *J. R. Stat. Soc. Ser. B* **32** 312–22

Taylor J A and Eckberg D L 1996 Fundamental relations between short-term RR interval and arterial pressure oscillations in humans *Circulation* **93** 1527–32

Triedman J K, Perrott M H, Cohen R J and Saul J P 1995 Respiratory sinus arrhythmia: time domain characterization using autoregressive moving average analysis *Am. J. Physiol.* **268** H2232–8

Turjanmaa V, Kalli S, Sydanmaa M and Uusitalo A 1990 Short-term variability of systolic blood pressure and heart rate in normotensive subjects *Clin. Physiol.* **10** 389–401

Victor R G and Mark A L 1985 Interaction of cardiopulmonary and carotid baroreflex control of vascular resistance in humans *J. Clin. Invest.* **76** 1592–8

Watanbe A and Stark L 1975 Kernel method for nonlinear analysis: identification of biological control system *Math. Biosci.* **27** 99–108

Wellstead P E and Edmunds J M 1975 Least-squares identification of closed-loop systems *Int. J. Contr.* **21** 689–99

Xiao X, Mukkamala R, Sheynberg N, Grenon S M, Ehrman M D, Mullen T J, Ramsdell C D, Williams G H and Cohen R J 2004 Effects of simulated microgravity on closed-loop cardiovascular regulation and orthostatic intolerance: analysis by means of system identification *J. Appl. Physiol.* **96** 489–97

Yana K, Saul J P, Berger R D, Perrott M H and Cohen R J 1993 A time domain approach for the fluctuation analysis of heart rate related to instantaneous lung volume *IEEE Trans. Biomed. Eng.* **40** 74–81